

Genomic analysis of organismal complexity in the multicellular green alga *Volvox carteri*

One-sentence Summary:

Analysis of the *Volvox carteri* genome reveals that this green alga's increased organismal complexity and multicellularity are associated with modifications in protein families shared with its unicellular ancestor, and not with large-scale innovations in protein coding capacity.

Authors and affiliations: Simon E. Prochnik,^{1*} James Umen,^{2*†} Aurora Nedelcu,³ Armin Hallmann,⁴ Stephen M. Miller,⁵ Ichiro Nishii,⁶ Patrick Ferris,² Alan Kuo,¹ Therese Mitros,⁷ Lillian K. Fritz-Laylin,⁷ Uffe Hellsten,¹ Jarrod Chapman,¹ Oleg Simakov,⁸ Stefan A. Rensing,⁹ Astrid Terry,¹ Jasmyn Pangilinan,¹ Vladimir Kapitonov,¹⁰ Jerzy Jurka,¹⁰ Asaf Salamov,¹ Harris Shapiro,¹ Jeremy Schmutz,¹¹ Jane Grimwood,¹¹ Erika Lindquist,¹ Susan Lucas,¹ Igor V. Grigoriev,¹ Rüdiger Schmitt,¹² David Kirk,¹³ Daniel S. Rokhsar^{1,7†}

* these authors contributed equally

† corresponding author

¹ U.S. Department of Energy, Joint Genome Institute, Walnut Creek, CA 94598, USA.

² The Salk Institute for Biological Studies, La Jolla, CA 92037, USA.

³ University of New Brunswick, Dept. of Biology, Fredericton, New Brunswick, Canada

⁴ Department of Cell. and Devel. Biol. of Plants, University of Bielefeld, Germany

5 Dept. Biological Sciences, University of Maryland, Baltimore County, Baltimore, MD 21250, USA.

6 Biological Sciences, Nara Women's University, Nara-shi, Nara Pref. 630-8506, Japan.

7 Center for Integrative Genomics, Dept. of Mol. and Cell Biol., UC Berkeley, Berkeley, CA 94720, USA.

8 EMBL, Heidelberg, Germany.

9 Faculty of Biology, University of Freiburg, Germany.

10 Genetic Information Research Institute, 1925 Landings Drive, Mountain View, CA 94043, USA.

11 HudsonAlpha Institute for Biotechnology, Huntsville, AL 35806, USA.

12 Genetics, University of Regensburg, D-93040 Regensburg, Germany.

13 Dept. Biology, Washington University in St. Louis, St. Louis, MO 63130, USA.

Abstract

The multicellular green alga *Volvox carteri* and its morphologically diverse close relatives (the volvocine algae) are uniquely suited for investigating the evolution of multicellularity and development. We sequenced the 138 Mb genome of *V. carteri* and compared its ~14,500 predicted proteins to those of its unicellular relative, *Chlamydomonas reinhardtii*. Despite fundamental differences in organismal complexity and life history, the two species have similar protein-coding potentials, and few species-specific protein-coding gene predictions. Interestingly, volvocine algal-specific proteins are enriched in *Volvox*, including those associated with an expanded and highly compartmentalized extracellular matrix. Our analysis shows that increases in organismal complexity can be associated with modifications of lineage-specific proteins rather than large-scale invention of protein-coding capacity.

Multicellularity and cellular differentiation evolved independently in diverse lineages including green and red algae, animals, fungi, plants, Amoebozoa and Chromalveolates (1)(Fig. S1A), yet the genetic changes that underlie these transitions remain poorly understood. The volvocine algae, which include both unicellular and multicellular species with various levels of morphological and developmental complexity, are an appealing model for studying such an evolutionary transition (2) (Fig. S2, supporting online text). Multicellular *Volvox carteri* (hereafter *Volvox*) has two cell types: ~2,000 small, biflagellate somatic cells that are embedded in the surface of a transparent sphere of glycoprotein-rich extracellular matrix (ECM), and ~16 large reproductive cells (termed gonidia) that lie just below the somatic cell monolayer (Fig. 1A, S1B,S2) (2). The somatic cells resemble those of *Chlamydomonas reinhardtii*, a model unicellular volvocine alga (3) (Fig. 1B). The evolutionary changes that produced *Volvox* from a *Chlamydomonas*-like unicellular ancestor have clear parallels in other multicellular lineages and took place more recently than in land plants and animals (4).

To begin to characterize the genomic features associated with volvocine multicellularity, we sequenced the 138 million base pair (Mbp) *Volvox* genome to ~11.1× redundant coverage (~2.9 million reads) using a whole genome shotgun strategy (5). The assembly captures over 98% of known mRNA sequences and ESTs (5). The *Volvox* nuclear genome is 19.6 Mbp (17%) larger than the *Chlamydomonas* genome (Table 1), primarily due to increased repeat content in *Volvox* relative to *Chlamydomonas* (5) (Table S1). While a few repeat families show bursts of expansion in the *Volvox* and *Chlamydomonas* lineages, most have changed gradually (Fig. S4) (5).

The sequence divergence between *Volvox* and *Chlamydomonas* is comparable to that between human and chicken (which diverged ~310 MYA), human and frog (~350 MYA) and *Arabidopsis* and poplar (~110 MYA) based on the frequency of synonymous transversions at

fourfold degenerate sites (4DTV distance) (5, 6)(Table S2). Although conserved synteny between *Volvox* and *Chlamydomonas* genomes is evident, the volvocine algae show higher rates of genomic rearrangement than vertebrates and eudicots (Tables S2-4, Fig. S5)

We predicted 14,566 proteins (at 14,520 loci) in *Volvox* (5) (Tables 1, S5-7). *Volvox* and *Chlamydomonas* have similar numbers of genes (Table 1)(3) and more than most unicells (Table S8). Genes in both algae are intron-rich (Table 1), like those of most multicellular organisms (Table S8), and introns are longer on average in *Volvox* (Fig. S6) (5). Novel protein domains and/or combinations are proposed to have contributed to multicellularity in metazoans (7) and such expansions are evident in both the plant and animal lineages (Fig. 2A, Table S9). In contrast, the numbers of domains and combinations in *Volvox* are very similar to those in *Chlamydomonas* and other unicellular species (Fig. 2A, Table S9) (5). microRNAs have been identified in *Chlamydomonas*, most of which have no homologs in *Volvox* (8, 9). It is likely that *Volvox* also possesses miRNAs, but these have yet to be characterized.

To investigate protein evolution in *Chlamydomonas* and *Volvox* we constructed families containing both orthologs and paralogs from twenty diverse species including animals, plants, fungi, protists and bacteria (5) (Table S10). We assigned 9,311 (64%) *Volvox* and 9,189 (63%) *Chlamydomonas* protein sequences to 7,780 families (Fig. 2B), of which 80% (5,423) contain one ortholog from each alga (Table S11). 1,835 families (26%) contain orthologs only from *Volvox* and *Chlamydomonas* (i.e. are volvocine-specific) (Fig 2B). Only 32 EST-supported *Volvox* gene models lack detectable homologs in *Chlamydomonas* or other species (5) (Tables S12, S13), suggesting that limited protein-coding innovation occurred in the *Volvox* lineage.

Gene family expansion or contraction is an important source of adaptive variation (10, 11). In a density plot of proteins per family in *Volvox* versus *Chlamydomonas* (Fig. 2C), most points lie

on or near the diagonal, showing that the majority of families have approximately equal membership from each alga. Exceptions include the gametolysin/VMP (*Volvox* matrix metalloprotease) family whose substrates are cell wall/ECM proteins (12) (Fig. 2C ‘g’), and a family containing leucine rich repeat proteins (LRRs) whose functions in green algae have not been well-defined (Fig. 2C, ‘L’). Conversely, families containing core histones and ankyrin repeats have more members in *Chlamydomonas* (Fig. 2C, ‘a’). In contrast, the subset of 1,835 volvocine-algae-specific families (5) shows a strikingly different distribution (Fig. 2D) with a significant bias towards more members in *Volvox* ($p=2E-120$, heterogeneity chi-squared test). These families include ECM proteins such as VMPs and pherophorins that both participate in ECM biogenesis (12), and an algal subgroup of cysteine proteases (Fig. 2D, ‘c’).

Although some of the genomic differences between *Volvox* and *Chlamydomonas* may reflect environmental adaptations that have not been extensively investigated (5), we expected many of the changes to be in protein families associated with the large differences in organismal complexity. Therefore, we investigated in detail pathways related to key developmental processes that are either novel or qualitatively different in *Volvox* relative to *Chlamydomonas* (2). These include: protein secretion and membrane trafficking (potentially involved in cytoplasmic bridge formation via incomplete cytokinesis (13, 14)), cytoskeleton (potentially involved in *Volvox*-specific basal body rotation, inversion and asymmetric cell division (15)), ECM and cell wall proteins (involved in ECM expansion, sexual differentiation and morphogenesis) (12) (Fig. S2) and cell cycle regulation (potentially involved in cell division patterning or asymmetric cell division). The components of these pathways are nearly identical in *Volvox* and *Chlamydomonas* (Table S14). Transcription-related proteins also have highly similar repertoires in the two species (Fig. S7, Table

S15) (5). Thus, with three noteworthy exceptions (see below), we found little difference in the complements of proteins that might underlie developmental complexity in *Volvox*.

The ECM comprises up to 99% of an adult *Volvox* spheroid and is larger and more structurally complex than the ancestral *Chlamydomonas*-like cell wall from which it was derived (12) (Fig. S3; supporting online text). These changes are mirrored by at least two dramatic changes in ECM protein family size in *Volvox* compared to *Chlamydomonas*, pherophorins (49 versus 27 members) and VMPs (42 versus 8 members) (Fig. 3A, S8, Table S14). We found expanded *Volvox*-specific clades of pherophorins and VMPs as well as species-specific duplications in both algae (Fig. 3A, S8). Besides their role in ECM structure, *Volvox* pherophorins have evolved into a diffusible sex-inducer glycoprotein that has replaced nitrogen deprivation (used in *Chlamydomonas* and other volvocine algae) as the trigger for sexual differentiation (16). The co-option of an ECM protein for sexual signaling shows parallels in the sexual agglutinins of *Chlamydomonas* that are themselves related to cell wall/ECM proteins (17). The *Volvox* ECM proteins pherophorins and VMPs diversified and then presumably were recruited to novel developmental roles in *Volvox*, thus representing a source of adaptive plasticity specific to the volvocine algae.

The *Volvox* and *Chlamydomonas* cell cycles are fundamentally similar, but *Volvox* has evolved additional regulation of timing, number, and types of cell divisions (symmetric and asymmetric) among different subsets of embryonic cells (2). The division program of males and females is further modified during sexual development to produce sperm and eggs (18). While most of the core cell cycle proteins of *Volvox* and *Chlamydomonas* have a 1:1 orthology relationship, the cyclin D family is notably larger in *Volvox*. In addition to three pairs of D-cyclins that have *Chlamydomonas* orthologs (cycd2, cycd3, cycd4), *Volvox* has four D1-related cyclins (cycd1.1-cycd1.4) whereas *Chlamydomonas* has only one (Fig. 3B). D cyclins bind cyclin-dependent kinases

and target them to phosphorylate retinoblastoma (RB)-related proteins (19). In *Chlamydomonas* the RB-related protein MAT3 controls the timing and extent of cell division (20), so it is plausible that the expanded D type cyclin family in *Volvox* plays a role in regulating its cell division program during development.

The genetic changes that brought about the evolution of multicellular life from unicellular progenitors remain obscure (2, 21, 22). For example, many proteins associated with animal multicellularity, such as cadherins and receptor tyrosine kinases (23) evolved in the unicellular ancestor of animals and are specific to its descendants. Other critical components of metazoan multicellularity, including key transcription factors and signalling molecules, are absent from the closest unicellular relatives of animals (22), suggesting that animal multicellularity also involved protein-coding innovation. Our comparisons of *Volvox* and *Chlamydomonas* indicate that with the interesting exceptions of pherophorins, VMPs and D cyclins, the developmental innovations in the *Volvox* lineage did not involve major changes in the ancestral protein repertoire. This is consistent with previous observations indicating co-option of ancestral genes into new developmental processes without changes in copy number or function (24-26). However, our analyses do suggest that expansion of lineage-specific proteins occurred preferentially in *Volvox* and provided a key source of developmental innovation and adaptation. Further studies of gene regulation (27) and the role of non-coding RNAs (28) will be enabled by the *Volvox* genome sequence, allowing a more complete understanding of the transformation from a cellularly complex *Chlamydomonas*-like ancestor to a morphologically and developmentally complex “fierce roller.”

References and Notes

1. S. L. Baldauf, *Science* **300**, 1703 (2003).
2. D. L. Kirk, *Bioessays* **27**, 299 (2005).
3. S. S. Merchant *et al.*, *Science* **318**, 245 (2007).
4. M. D. Herron, J. D. Hackett, F. O. Aylward, R. E. Michod, *Proc Natl Acad Sci U S A* **106**, 3254 (2009).
5. Materials and methods are available as supporting material on Science Online.
6. R. R. Reisz, J. Muller, *Trends Genet* **20**, 237 (2004).
7. N. H. Putnam *et al.*, *Science* **317**, 86 (2007).
8. T. Zhao *et al.*, *Genes Dev* **21**, 1190 (2007).
9. A. Molnar, F. Schwach, D. J. Studholme, E. C. Thuenemann, D. C. Baulcombe, *Nature* **447**, 1126 (2007).
10. O. Lespinet, Y. I. Wolf, E. V. Koonin, L. Aravind, *Genome Res* **12**, 1048 (2002).
11. J. Zhang, *Trends Ecol Evol* **18**, 292 (2003).
12. A. Hallmann, *Int Rev Cytol* **227**, 131 (2003).
13. K. J. Green, D. L. Kirk, *J Cell Biol* **91**, 743 (1981).
14. K. J. Green, G. I. Viamontes, D. L. Kirk, *J Cell Biol* **91**, 756 (1981).
15. D. Kirk, *Volvox: Molecular-genetic origins of multicellularity and cellular differentiation*. (Cambridge University Press, Cambridge, 1998).
16. A. Hallmann, *Plant J* **45**, 292 (2006).
17. P. J. Ferris *et al.*, *Plant Cell* **17**, 597 (2005).
18. P. Ferris *et al.*, *Science* **328**, 351 (2010).
19. L. De Veylder, T. Beeckman, D. Inze, *Nat Rev Mol Cell Biol* **8**, 655 (2007).
20. S. C. Fang, C. de los Reyes, J. G. Umen, *PLoS Genet* **2**, e167 (2006).
21. L. W. Buss, *The Evolution of Individuality*. (Princeton University Press, Princeton, 2006), pp. 224.
22. N. King *et al.*, *Nature* **451**, 783 (2008).
23. N. King, C. T. Hittinger, S. B. Carroll, *Science* **301**, 361 (2003).
24. S. M. Miller, D. L. Kirk, *Development* **126**, 649 (1999).
25. I. Nishii, S. Ogihara, D. L. Kirk, *Cell* **113**, 743 (2003).
26. Q. Cheng, R. Fowler, L. W. Tam, L. Edwards, S. M. Miller, *Dev Genes Evol* **213**, 328 (2003).
27. S. B. Carroll, *Cell* **134**, 25 (2008).
28. K. J. Peterson, M. R. Dietrich, M. A. McPeek, *Bioessays* **31**, 736 (2009).
29. The work conducted by the U.S. Department of Energy Joint Genome Institute is supported by the Office of Science of the U.S. Department of Energy under Contract No. DE-AC02-05CH11231 and by NIH R01 GM078376 and Copen Foundation to JU; Natural Sciences and Engineering Research Council – Canada to AN; NSF IBN-0444896 and IBN- 0744719 to SMM, NIH 5 P41 LM006252 to VK. We thank M. Cipriano for Pfam annotations; E. Hom, E. Harris, and M. Stanke for Augustus u9 gene models and R. Howson for artwork. Sequence data from this study are deposited at DDBJ/EMBL/GenBank under the project accession ACJH00000000.

Supporting Online Material

Supporting Materials and Methods S1A-S1R

Supporting Text S2A-D

Figs S1-S8

Tables S1-16

Figure legends

Fig. 1: *Volvox* and *Chlamydomonas*. (A) Adult *Volvox* comprise ~2,000 *Chlamydomonas*-like somatic cells (s) and ~16 large germ-line gonidia (g) (bar = 200 μ m)(see also Fig. S1B); (B) *Chlamydomonas* cell showing apical flagella (f), chloroplast (c) and eyespot (e) (bar = 10 μ m). Microscopy described in (5).

Fig. 2: Comparisons of protein domains and families. (A) Total number of Pfam domains in the multicellular (green) and unicellular (blue) species: *Chlamydomonas* (cre); *Volvox carteri* (vca); *Arabidopsis thaliana* (ath); *Thalassiosira pseudonana* (tps); *Phaeodactylum tricornutum* (ptr); *Monosiga brevicollis* (mbr); *Nematostella vectensis* (nve); and *Homo sapiens* (hsa). (B) The numbers of protein families from *Volvox*, *Chlamydomonas* and other species (5) are shown in a Venn diagram. The number of *Volvox* and *Chlamydomonas* members per protein family are plotted for all families (C) and for the volvocine-algae-specific subset (D). In these density plots, the position of each square represents the number of family members in *Volvox* (x axis) and *Chlamydomonas* (y axis), with coloring to indicate the total number of families plotted at each position. The Pfam domains for outlier families are abbreviated as: a Ankyrin repeat, c cysteine protease, g gametolysin, h histone, L Leucine rich repeat.

Fig 3: Diversification of key protein families with known or predicted roles in *Volvox* development.

Unrooted maximum likelihood trees (5) are shown for pherophorins (A) and cyclins (B). Protein sequences are from *Volvox* (Vc; green) and *Chlamydomonas* (Cr; blue). Incomplete gene models were not included ; *Volvox*-specific clades with poorly-resolved branches are collapsed into triangles; bootstrap support $\geq 50\%$ is indicated on branches. Red asterisks indicate pherophorins whose mRNA levels are up-regulated by sex inducer (16).

Table 1: Comparison of the *Volvox* and *Chlamydomonas* genomes.

Group	Species	Genome Size (Mbp)	Number of chromosomes	%GC	Protein coding loci	% coding	% genes with introns	Introns per gene	Median intron length (bp)
CHLOROPHYTA	<i>Volvox carteri</i>	138	14*	56	14,520	18.0	92	7.05	358
	<i>Chlamydomonas reinhardtii</i>	118	17	64	14,516	16.3	91	7.4	174

* see (15)

Fig. 1

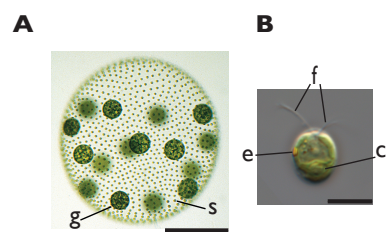
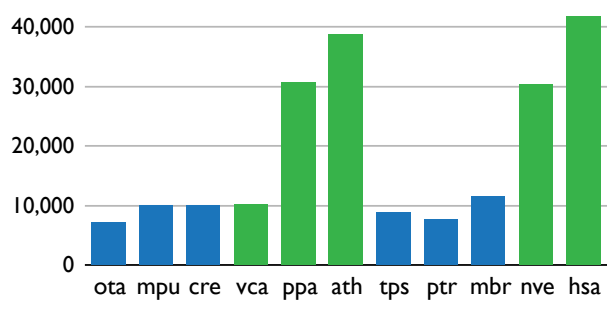
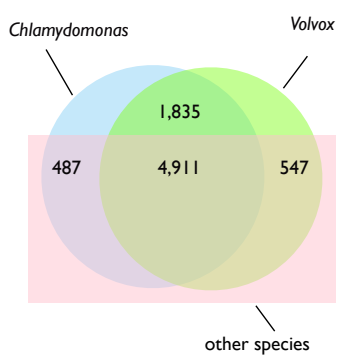


Fig. 2

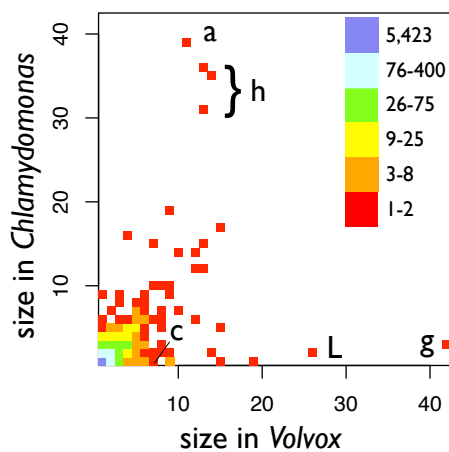
A



B



C



D

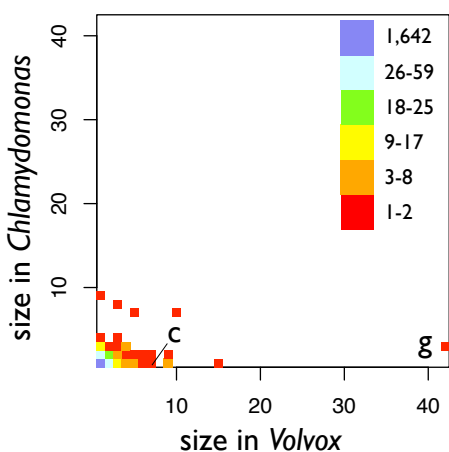
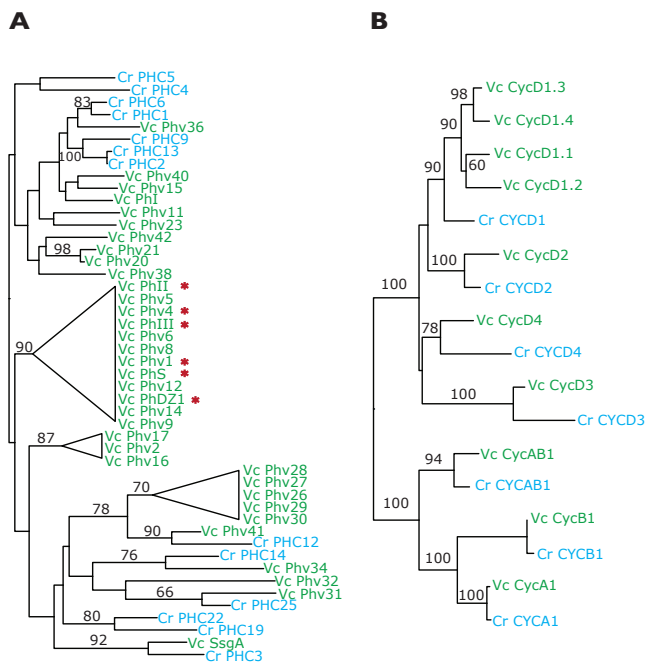


Fig. 3



Supplemental Online Material for the Genomic analysis of organismal complexity in the multicellular green alga *Volvox carteri*

Table of Contents

1) MATERIALS AND METHODS	3
A. Nuclear genome sequencing and assembly	3
B. Comparison and annotation of repeats in <i>Volvox</i> and <i>Chlamydomonas</i>	4
B1. Overview of repeat analysis	4
B2. Analysis of satellite repeats in <i>Volvox</i> and <i>Chlamydomonas</i>	5
B3. Generation annotation and filtering of RepeatScout Libraries	5
C. Analysis of repeat expansions	7
D. Calculation of corrected 4-fold degenerate transversion (4DTV) distances	7
E1. Synteny and genomic rearrangements	8
E2. Definition of C-score	9
F. Loss of synteny through genomic rearrangements	9
G. cDNA library construction and EST sequencing	10
H. Prediction of gene models	11
I. <i>Volvox</i> has longer introns than <i>Chlamydomonas</i>	13
J. Pfam protein domain assignments	13
K. Pfam domain combinations unique to <i>Chlamydomonales</i>	13
L. Pfam domain combinations specific to <i>Volvox</i> or specific to <i>Chlamydomonas</i> or both	14
M. Construction of protein families	14
N. <i>Volvox</i> -specific genes	15
O. <i>Chlamydomonas</i> -specific genes	16
P. Volvocene algae-specific protein families	16
Q. Analysis of Transcription Associated Proteins	17
R. Annotation of genes associated with developmental biological processes in <i>Volvox</i>	19
Membrane trafficking proteins	19
Cell cycle proteins	19
Cytoskeletal proteins	20
Cell wall and extracellular matrix proteins	20
Phylogenetic analyses	20
2) SUPPORTING TEXT	22
A. Volvocene algae as a model for the evolution of multicellularity	22
B. The <i>Volvox</i> vegetative life cycle	23
C. The <i>Volvox</i> sexual cycle	23
D. The <i>Volvox</i> ECM	23
E. Environmental adaptations of <i>Volvox</i> and <i>Chlamydomonas</i>	24
3) SUPPLEMENTAL FIGURES	25
Fig. S1: <i>Volvox</i> phylogeny, morphology and development	25
Fig. S2: The algae of the volvocene lineage	27
Fig. S3: Schematic diagram of ECM in <i>Volvox</i>	29
Fig. S4: Histograms of Jukes-Cantor distance between repeats	31
Fig. S5: Synteny dotplot between <i>Volvox</i> and <i>Chlamydomonas</i> genomes	33
Fig. S6: Intron lengths in <i>Volvox</i> and <i>Chlamydomonas</i>	35
Fig. S7: Scatter plot of family size in transcription associated proteins	37
Fig. S8: Diversification of <i>Volvox</i> matrix metalloprotease family	39
4) SUPPLEMENTAL TABLES	41

Table S1: Summary of repeats in <i>Volvox</i> and <i>Chlamydomonas</i> genomes	41
Table S2: Genome evolution in green algae, animals, plants and diatoms.....	42
Table S3: Counts of filtered genes that were used to build syntenic blocks.....	42
Table S4: Counts of <i>Volvox</i> and <i>Chlamydomonas</i> genes making up syntenic blocks with selected numbers of intervening genes allowed for real and scrambled gene order.....	42
Table S5: Counts of gene models predicted in <i>Volvox</i> by initial automated annotation, classified by method	43
Table S6: EST and homology evidence supporting initial <i>Volvox</i> and <i>Chlamydomonas</i> gene models	44
Table S7: Gene structure statistics of <i>Volvox</i> and <i>Chlamydomonas</i> gene models.....	44
Table S8: Comparison of <i>Volvox</i> genome statistics to selected other genomes.	45
Table S9: Pfam domain counts and combinations in <i>Volvox</i> and <i>Chlamydomonas</i> compared to selected other species.....	46
Table S10: Complete predicted protein sets used to build protein families.....	46
Table S11: Protein family size distribution in <i>Volvox</i> and <i>Chlamydomonas</i>	48
Table S12: <i>Volvox</i> -specific gene models with EST evidence.....	48
Table S13: <i>Chlamydomonas</i> -specific gene models with EST support.....	49
Table S14: Proteins involved in processes that are associated with increased developmental complexity in <i>Volvox</i> relative to <i>Chlamydomonas</i>	49
Table S15: Predicted numbers of TAPs	55
Table S16: Summary of RepeatScout libraries	58
5) SUPPLEMENTAL REFERENCES	59

1) MATERIALS AND METHODS

A. Nuclear genome sequencing and assembly

We prepared high quality genomic DNA from a vegetative culture of female *Volvox carteri* f. *nagariensis*, Eve (S1), a subclone of HK10 (S2, 3), which is a standard female lab strain of *Volvox carteri* (hereafter *Volvox*) that was originally isolated in 1965 by Richard Starr from a pond associated with a rice paddy near Kobe, Japan. The genomic DNA was prepared by a standard protocol involving CsCl gradient banding to separate it from RNAs (S1), but it could not be separated from chloroplast and mitochondrial DNA. The genome sequences of these two organelles have already been determined (S4).

Paired-end whole-genome shotgun (WGS) sequencing (S5) of three libraries with insert sizes of 2-3 kb (AOBN); 6-8 kb (ABSY) and 35-40 kb (AOBO) generated 1,430,397, 1,269,395 and 230,112 reads respectively, covering 1,361, 1,310 and 235 Mb raw sequence respectively, together totaling 2,906 Mb of raw sequence. The reads were screened for vector sequence using Cross_match (S6) and trimmed for vector and low quality sequences. Reads shorter than 100 bases after trimming were excluded from the assembly leaving 1,343,753 2-3 kb insert reads (94%, 836 Mb of sequence); 1,207,057 6-8 kb insert reads (95% 760 Mb) and 224,372 35-40 kb insert reads (98%, 113 Mb).

The filtered and trimmed read sequences were assembled using JAZZ 1.0.3 (S7). A word size of 14 was used for seeding alignments between reads. The ‘unhashability threshold’ parameter was set to 40, meaning that words present over 40 times in the data set were not used to seed alignments. A mismatch penalty of -30.0 was used that generally allows assembly of sequences that are more than ~97% identical.

The initial assembly contained 147.4 Mb of scaffold sequence, of which 12.5 Mb (8.5%) was gaps. There were 7,391 scaffolds, with a scaffold N50/L50 of 35/1.41 Mb, and a contig N50/L50 of 795/42.7 kb. Scaffolds < 1 kb long as well as redundant scaffolds (those scaffolds shorter than 5kb long with >80% identity to another scaffold whose length was greater than 5kb) were removed from the assembly. This left 141.5 Mb of scaffold sequence, of which 12.4 Mb (8.8%) was gaps. The filtered assembly contained 1,327 scaffolds, with a scaffold N50/L50 of 33/1.50 Mb, and a contig N50/L50 of 729/45.4 kb. The sequence depth derived from the assembly was 11.1 ± 0.2 .

To estimate the completeness of the assembly with respect to transcribed genes, 72 *Volvox* mRNAs that were known prior to the genome project were downloaded from the nr database at NCBI (S8) and aligned to the assembly using BLAT (S9) with default parameters. All 72 mRNAs had hits to the assembly with >97% identity over most of their lengths.

As a second test of completeness relative to transcribed loci, we considered 129,528 dideoxy-sequenced ESTs that had $\leq 40\%$ of unmasked sequence after removal of low complexity and simple repeat regions (see below). Of these ESTs, 127,056 (98.0%) aligned to the assembly with BLAT (S9) ($>90\%$ identity over $>50\%$ of their length). The 2,472 filtered ESTs that did not align to the genome were examined further. Approximately 1/3 (857) had hits with BLASTX (S10) (E-value $< 1e-10$) to known proteins from the UniProt database (S11). These included 408 ESTs (48% of unmapped ESTs with hits) with best hits to proteins annotated as “ribosomal protein” and 93 ESTs (11% of unmapped ESTs with hits) so annotated as related to chlorophyll binding. We do not rule out the possibility that these and other unmapped ESTs are derived from loci not included in the genome assembly because they are embedded in repetitive sequence. Overall, we can conservatively estimate that the completeness of the *Volvox* genome assembly with respect to transcribed loci captured by ESTs is likely better than 98%.

B. Comparison and annotation of repeats in *Volvox* and *Chlamydomonas*

B1. Overview of repeat analysis

The *Volvox* genome assembly is 19,621,448 bp longer than that of *Chlamydomonas reinhardtii* (hereafter *Chlamydomonas*) (Table 1). We compared the repeat content of the two genomes to determine the contribution made by repeats to the difference in genome size. To do this, we built and annotated a custom repeat library for each algal genome and ran RepeatMasker (S12) on each assembly with the appropriate custom repeat library and the ‘-gcalc’ option (Table S1).

The custom *Volvox* repeat library was assembled from five component libraries:

- i) 45 *Volvox carteri*-specific and 72 *Chlamydomonas*-specific repeat sequences from RepBase (20080611 update) (S13);
- ii) 147 sequences that had been generated by analysis of the *Chlamydomonas* genome (S14);
- iii) 33 repeat elements from the *Volvox* assembly that were generated using the same approach as had been used previously for the *Chlamydomonas* genome (S14). (We estimate the curated set from the *Volvox* genome is 20-25% complete);
- iv) a library of 1,704 satellite repeat sequences (with lengths ranging from 20 to 1,162 bp) built by searching the whole genome shotgun reads for over-represented 16-mers and assembling overlapping 16-mers (as described below), and

v) 1,511 repeats identified by RepeatScout (S15) (Table S16). The repeat sets were annotated and filtered leaving 1,449 sequences (as described below).

In parallel, a custom *Chlamydomonas* repeat library was assembled from:

- i) *Volvox*- and *Chlamydomonas*-specific repeat sequences from RepBase (20080611 update) (S13);
- ii) 147 *Chlamydomonas* repeat sequences identified as in ii) above;
- iii) 33 *Volvox* repeats identified as in iii) above;
- iv) a library of 100 satellite sequences (with lengths 25, 92, 107, 181 or 184 bp) (see below) and
- v) 1,057 repeats identified by RepeatScout. After filtering the library contained 1,013 repeats (Table S16 and see below).

B2. Analysis of satellite repeats in *Volvox* and *Chlamydomonas*

A library of all 16 nt long sequences (16-mers) that occur at least 500 times was generated from approximately half the WGS reads (all reads from the AOBN library). 16-mers that overlap each other were assembled into longer sequences by repeatedly looking for 15 nt overlaps and extending by a single nucleotide overhang until either no further extensions were possible (in which case extensions in the opposite direction were explored) or the sequence looped back on itself. Both the sequences that could not be extended further and the circular sequences were added to the library of putative satellite sequences as long as they were at least 20 nt long.

B3. Generation annotation and filtering of RepeatScout Libraries

Generation of libraries of repeats with RepeatScout (S15) and their subsequent filtering and annotation was accomplished as follows. First, RepeatScout was run on the *Volvox* assembly. This produced a library of 1,511 repeat sequences (Table S16). Next RepeatScout was run on the *Chlamydomonas* assembly, generating 1,057 sequences. The repeat sequences in these two libraries were classified as described in the set of rules below.

To annotate and filter repeat sequences in the RepeatScout libraries generated from the *Volvox* and *Chlamydomonas* genomes, we first masked the *Volvox* genome with the 1,511 sequence RepeatScout library using RepeatMasker (S12) with the '-gccalc' option. We then counted the number of times each repeat sequence hit the genome. We also counted the percentage of repeat instances in the genome that also overlapped gene models and ESTs by two criteria: ≥ 200 nt length and $\geq 80\%$ of the length of the repeat. Sequences in the repeat library were

assigned Pfam domains by running HMMPFAM, part of the HMMER package (S16), on the library with an E-value cutoff of 1E-5. Repeat sequences with Pfam domain assignments were sub-divided into those with a TE-associated Pfam (PF00075, PF00078, PF00665, PF03372, PF03732, PF07727, PF01527) and those with non-TE associated Pfam domains (all other Pfam domains). We also ran tRNAscan-SE (S17) on the repeat sequences.

To assign TE classes to sequences in the *Volvox* RepeatScout library that have homology to known TE classes, we ran RepeatMasker on the *Volvox* RepeatScout library with each of two repeat libraries (as these two libraries contain partially overlapping sequences): in the first run, the custom library of repeats that we had curated manually (see above) was used to mask the RepeatScout repeat library; in the second run, RepeatMasker was run with the option ‘-species chlamydomonodales’ to use the volvocine algae repeat sequences in the 20080611 release of RepBase Update (S13). In cases where the longest repeat that masked a RepeatScout library sequence was in the class ‘Simple_repeat’ or ‘Low_complexity’, this annotation was ignored as RepeatMasker has dedicated algorithms for finding repeats of these two classes that are based solely on sequence composition, rather than homology to known TEs. In cases where the longest annotation in the RepeatScout repeat sequence was not a Simple_repeat or non Low_complexity-repeat, the repeat sequence was assigned the class ‘Complex_repeat’. If the RepBase Update library found a complex repeat and our curated library did not, then the complex repeat that was found was used for the classification.

For all the sequences still without a ‘Complex_repeat’ classification, in which either RepeatMasker detected a tRNA in the sequence or tRNAscan-SE predicted a tRNA with score > 22 and the length of the repeat < 120 nt, the repeat was given the classification ‘tRNA’.

Sequences were classified as ‘Satellite’ or ‘rRNA’ if RepeatMasker assigned either of these classifications to a sequence.

Sequences that still had not been given a classification and also had Pfam domains were classified ‘non_TE_PFAM’ if the Pfam domain is not associated with TEs or ‘TE_associated_PFAM’ if the Pfam domain is associated with TEs (see above).

122 repeat sequence that still had not been classified met all of the following three criteria and we therefore reasoned that these repeat may be novel and classified them as ‘Putative_novel’ (Table S16). The three criteria were:

- i) either there were no instances of the repeat sequence in the genome that overlapped an EST by at least 200 bp or no instances in the genome that overlapped an EST by at least 80% of the length of the repeat sequence;

- ii) either there were no instances of the repeat sequence in the genome that overlapped a gene model by at least 200 bp or no instances in the genome that overlapped a gene model by at least 80% of the length of the repeat sequence; and
- iii) the length of the repeat was over 500 nt.

The remaining 911 sequences were classified ‘Unknown’. To see if these unknown repeats could be classified further, InterProScan (S18) was run on the 911 sequences to assign Pfam domains using specific gathering thresholds for each HMM. This is more accurate than using a single E-value cutoff for all domains. Hits were manually inspected and 62 sequences with Pfams that are not associated with TEs were deleted from the RepeatScout library. This left 1,449 (Table S16).

A parallel analysis in *Chlamydomonas* starting with a RepeatScout library of 1,057 sequences produced a filtered and annotated set of 1,103 sequences (Table S16)

C. Analysis of repeat expansions

The *Volvox* genome was masked with RepeatMasker using the RepeatScout library (see above), which was annotated as described above. All repeat sequences in the *Volvox* genome longer than 500 nt and belonging to a known class of TE were collected and their Jukes-Cantor distance, corrected for multiple substitutions ($K = -3/4 \times \ln(1-4i/3)$, where i is percent nucleotide dissimilarity from the repeat consensus) from the RepeatScout consensus repeat sequence were plotted in a histogram (Fig. S4A-C). A parallel analysis was performed for *Chlamydomonas* (Fig. S4D-E).

Bursts of TE expansion appear as secondary peaks in the histogram to the right of the descending curve that starts at a Jukes-Cantor distance of zero. No secondary peaks are apparent in the total repeat histograms for *Volvox* or *Chlamydomonas* (Fig S4A,4D), but they are present in plots for specific TE families such as Gypsy and Copia in *Chlamydomonas* (Figs. S4E,4F).

D. Calculation of corrected 4-fold degenerate transversion (4DTV) distances

The frequency of transversions at the third position of four-fold degenerate codons (4DTV) can be used to measure the rate of neutral evolution as these transversions do not change the amino acid that is encoded. We calculated 4DTV distances between orthologous protein sequences in pairs of genomes using a previously described method (S19). Briefly, we identified a set of mutual best BLASTP hits (MBH) between all predicted proteins in each pair of species and used them to align coding regions. The number of transversions at conserved

four-fold degenerate sites divided by the total number of four-fold degenerate sites gives the 4DTV frequency. This raw calculation is then corrected for multiple substitutions using the formula $4DTV_C = -1/2\ln(1-2 \times 4DTV_U)$, where $4DTV_C$ is the corrected 4DTV and $4DTV_U$ the uncorrected 4DTV.

E1. Synteny and genomic rearrangements

Synteny dotplots for *Volvox-Chlamydomonas* and human-chicken are shown in Fig. S5 and reveal the extent of conserved gene order.

We used the updated *Volvox* v2 assembly (<http://genome.jgi-psf.org/Volca1/Volca1.download.ftp.html>) and the *Chlamydomonas* v4 assembly (<http://www.phytozome.net/chlamy>) for the following analysis of synteny between *Volvox* and *Chlamydomonas*. The *Chlamydomonas* v4 assembly has 17 chromosomes and 61 minor scaffolds; the *Volvox* v2 assembly has 434 scaffolds (compared to 1,265 for v1).

At the time of analysis, neither the *Volvox* v2 assembly nor the *Chlamydomonas* v4 assembly had been annotated with gene model annotations so we mapped *Volvox* v1 and *Chlamydomonas* v3.1 transcripts to their respective updated assemblies using blat (S9) with default parameters and taking the best hit to the assembly. After mapping and filtering (see below), 4,349 of the 4,804 (91%) *Volvox* gene models were on scaffolds containing 25 or more genes, permitting useful synteny analysis.

Syntenic segments were constructed between pairs of genomes as follows. We only considered the longest gene model at any locus because the commonest problem with gene prediction for a genome with incomplete EST coverage is truncation.

- 1) Gene models whose translations did not have a WU-BLASTP (S10) hit to the other proteome (E-value < 1E-10) were removed.
- 2) Tandem expansions were collapsed: if two or more neighboring genes encode similar proteins (WU-BLASTP E-value < 1E-10) and had no more than 2 intervening genes, only the longest gene model of the two or more similar, neighboring, genes was retained as a representative of the duplication.
- 3) Gene models whose best hit to the other proteome had a C-score (see below) less than 0.8 were removed.
- 4) Gene models with more than 10 hits (E-value < 1E-10) to the other proteome were removed because large gene families can seed false synteny blocks in many different genomic locations.

5) The remaining gene models were ordered along chromosomes (or scaffolds in the case of the *Volvox* assembly). The chromosomes/scaffolds in Fig. S5 were arranged in decreasing order of the numbers of gene models contained. In multiple iterations, the gene models were used to seed synteny blocks (defined as containing two or more genes with conserved gene order) in each genome with different numbers of intervening genes in the range zero to ten being picked in each iteration (data from zero to four intervening genes are shown in Table S4).

6) As the number of intervening genes allowed between two genes in a synteny block increases, so does the chance of finding such blocks by chance. In order to establish a “null” model for each condition the order of the filtered genes was scrambled and the number of synteny blocks formed with different number of intervening genes was determined (Table S4).

The number of genes remaining in synteny blocks after this filtering process is shown in Table S3. A comparison of the synteny dotplots of *Volvox* vs. *Chlamydomonas* (Fig. S5A) and human vs. chicken (Fig. S5B) shows that the human-chicken genes tend to lie on longer (up to whole chromosome arm) synteny segments than in the two algae. Furthermore, the synteny blocks that are present in the algae are broken up by micro-inversions to a greater extent. Overall, there has been less overall rearrangement in vertebrates (Fig. S5B) than in *Volvox-Chlamydomonas* Fig. S5A.

Where whole genome duplication (WGD) has taken place, it is visible in plots of this type as repeated diagonal stretches in a row or column. There is no evidence of WGD in *Volvox*, *Chlamydomonas*, or their common ancestor (Fig. S5), unlike yeasts, higher plants and metazoans (S20) where WGDs have played a significant role in genome evolution.

E2. Definition of C-score

We used the metric C-score as a measure of similarity between a protein from one predicted proteome and the proteins from a second predicted proteome. The C-score for protein X in one species and protein Y in a second species (C_{XY}) is defined as the BLAST score of X against Y divided by the best BLAST score for protein X against all of the proteins in species Y. The C-score can be used to detect the presence of both orthologs (defined as mutual best BLAST hits) as well as potential paralogs. If X and Y are mutual best hits, then C_{XY} and C_{YX} will both equal 1. Recent paralogs of X will have a C-score of slightly less than 1 relative to Y; similarly, recent paralogs of Y will have a C-score of slightly less than 1 relative to X.

F. Loss of synteny through genomic rearrangements

To quantify the amount of rearrangement on the gene by gene scale, we used the following metric: we calculated the fraction of all pairs of neighboring synteny

orthologs from each set of two genomes (ascertained in the previous section) that were not adjacent to each other in the other genome in the pair, reasoning that this would have been caused by a rearrangement since the two genomes diverged (Table S2).

G. cDNA library construction and EST sequencing

We extracted total RNA from *Volvox carterif. nagariensis* female strains Eve and Eve10 and male strain 69-1b. For Eve and 69-1b, we extracted RNA from samples 1.5, 10, 24, 48 hours after sexual-induction and pooled the samples. For Eve10, we extracted RNA from 2-4 and 32-128 cell stages and pooled the samples. Poly A⁺ RNA was isolated from total RNA using the Absolutely mRNA Purification kit and manufacturer's instructions (Stratagene, La Jolla, CA). cDNA synthesis and cloning used a modified procedure based on the "SuperScript plasmid system with Gateway technology for cDNA synthesis and cloning" (Invitrogen, Carlsbad, CA). 1-2 µg of poly A⁺ RNA, SuperScript II reverse transcriptase (Invitrogen) and oligo dT-*NotI* primer (5' GACTAGTTCTAGATCGCGAGCGGCCGCCCT₁₅VN 3', where V is any nucleotide except T and N is any nucleotide) were used to synthesize first strand cDNA. Second strand synthesis was performed with *E. coli* DNA polymerase I, DNA ligase, and RNaseH followed by end repair using T4 DNA polymerase. An adaptor including the overhanging pre-cut *SalI* site at the 5' end (5' TCGACCCACGCGTCCG 3' and 5' CGGACCGCGTGGG 3') was ligated to the cDNA that was then digested with *NotI* (New England BioLabs, Ipswich, MA), and size selected by gel electrophoresis (1.1% agarose). The cDNA inserts were ligated into the *SalI* and *NotI* digested vector pCMVsport6 (Invitrogen). The ligation was transformed into ElectroMAX T1 DH10B cells (Invitrogen). In total, five cDNA libraries were constructed.

Library quality was assessed in two ways. First we ensured that the number of clones without inserts was less than 10% by randomly selecting 24 clones and PCR amplifying the cDNA inserts with the primers M13-F (5' GTAAAACGACGGCCAGT 3') and M13-R (5' AGGAAACAGCTATGACCAT 3'). Second, a test production run of a single 384-well plate was undertaken (as described below) and sequence quality, diversity and length were investigated. For the main production run, cells from each library were plated onto agarose plates (254 mm plates from Teknova, Hollister, CA) at a density of approximately 1,000 per plate. Plates were grown at 37°C for 18 hours then individual colonies were picked and each used to inoculate a well containing LB media with appropriate antibiotic in a 384 well plate (Nunc, Rochester, NY). Clones were grown in selective media in 384 well plates and plasmid DNA for sequencing was produced by rolling circle amplification (S21) (Templiphi, GE Healthcare, Piscataway, NJ). Inserts were sequenced from both ends using primers complimentary to the flanking vector sequence with the following sequences: Fwd: 5' ATTTAGGTGACACTATAGAA and Rev: 5' TAATACGACTCACTATAGGG)

and Big Dye terminator chemistry on ABI 3730 DNA Analyzers (ABI, Foster City, CA). We generated pairs of reads (from both 5' and 3' ends of each cDNA clone), generating 42,240, 51,456 and 72,192 reads from Eve, Eve10 and 69-1b respectively, giving a grand total of 165,888 ESTs (Expressed Sequence Tags).

All 165,888 ESTs were processed through the JGI EST pipeline. Phred (S6, 22) was used to call bases and generate quality scores. Vector, linker, adapter, poly-A/T, and other artifact sequences were removed using the Cross_match software (S6, 22) and an internally-developed short pattern finder. Low quality regions of the read were identified using internally-developed software, masking regions with a combined quality score of less than 15. The longest high quality region of each read was considered to be the sequence of the EST. ESTs shorter than 150 bp as well as those containing common contaminating sequences from e.g. *E. coli*, common vectors, and sequencing standards were removed from the data set. After these filtering steps, 132,038 ESTs were left (33,407, 37,354, and 61,277 from Eve, Eve10 and 69-1b respectively. An additional 2,510 ESTs were not included in the analysis of assembly completeness (see above) due to their having > 40% low complexity and repetitive sequence as determined by mdust (S23) run with the '-v 20' setting. This left 129,528 ESTs for consideration in analysis of assembly completeness.

Clustering the EST sequences involved first generating all-by-all pairwise alignments between the 132,0338 filtered reads. ESTs sharing an alignment of at least 98% identity were then assigned to the same cluster. In addition, ESTs not sharing alignments but derived from opposite ends of the same cDNA clone were assigned to the same cluster. Clusters of ESTs were assembled into consensus sequences, contigs or singlets using CAP3 (S24). A total of 16,569 assembled consensus sequences were generated.

H. Prediction of gene models

The 1,265 *Volvox* v.1 scaffolds were masked using RepeatMasker (<http://www.repeatmasker.org/>) and a library of 1,015 transposable elements (TEs), including manually curated *Volvox* and *Chlamydomonas* TEs (<http://www.girinst.org/>).

After masking, the JGI annotation pipeline was used to generate gene models. This pipeline employs gene prediction programs that are based on a variety of methods, as follows:

- 1) *ab initio* methods (FGENESH; <http://www.softberry.com/>);
- 2) homology-based methods (FGENESH+ and Genewise; <http://www.ebi.ac.uk/Wise2/>) seeded by Blastx alignments against sequences of nr, IPI (<http://www.ebi.ac.uk/IPI/>), and JGI *Chlamydomonas* annotation v3 (<http://www.jgi.doe.gov/chlamy/>);

- 3) cDNA-based methods (EST_map; <http://www.softberry.com/>) seeded by 13,722 EST cluster consensus sequences derived from 87,866 *Volvox* ESTs. At the time the JGI annotation pipeline was run, 87,593 sequences had already been sequenced by the JGI (see above). The remaining 273 EST sequences were downloaded from the nr database at GenBank (S8);
- 4) synteny-based methods (FGENESH-2; <http://www.softberry.com/>) using the JGI *Chlamydomonas* assembly and annotation (<http://www.jgi.doe.gov/chlamy/>).

Genewise models were completed using scaffold data to find start and stop codons. EST clusters were used to extend, verify, and complete the predicted gene models. The resulting set of models was then filtered for the “best” models, based on criteria of completeness, length, EST support, and homology support, to produce a non-redundant representative set. This representative set was subject to protein functional analysis and manual curation, as described in the next sections.

The function of the translations of the predicted gene models was predicted using TMHMM (<http://www.cbs.dtu.dk/services/TMHMM/>), InterProScan (<http://www.ebi.ac.uk/interpro/>), and hardware-accelerated double-affine Smith-Waterman alignments (http://www.timelogic.com/decypher_sw.html) against SwissProt (<http://www.expasy.org/sprot/>), KEGG (<http://www.genome.jp/kegg/>), and KOG (<http://www.ncbi.nlm.nih.gov/COG/>). Finally, KEGG hits were used to map EC numbers (<http://www.expasy.org/enzyme/>), and Interpro and SwissProt hits were used to map GO terms (<http://www.geneontology.org/>).

We initially predicted 15,544 gene models in the genome of *Volvox*. 23% of these gene models were seeded by alignments of proteins in nr against the *Volvox* genome, while 67% were predicted *ab initio* and 10% were seeded using synteny with *Chlamydomonas reinhardtii* gene models (Table S5). Complete models with start and stop codons comprise 85% of the 15,544 initial gene predictions; 34% are consistent with ESTs and 70% align with proteins in Swissprot (<http://www.expasy.org/sprot/>) (Table S6).

The average *Volvox* gene is 5.27 kb long, the average gene density is 113 genes/Mb, and the average transcript has 7.78 exons (Table S7). The average protein length is 558 aa. We predicted that 4% of the proteins possess at least one transmembrane domain, 30% possess a signal peptide, and 2% possess both. We assigned 1,757 distinct GO terms to 4,566 proteins (30%), and we assigned 3,062 proteins (20%) to KEGG pathways, totaling 625 distinct EC numbers. We assigned 9,889 proteins (64%) to 3,145 distinct KOGs.

Knowing that the repeat masking was incomplete, as a last step, we filtered the initial set of 15,544 gene models, removing all those that encoded proteins with homology to transposable elements or were assigned TE-associated Pfam domains by InterProScan (S18). 1,103 protein models were removed from the set of 15,544, leaving 14,520 (Table S6).

Web-based editing tools available at the JGI genome portal were used to examine and improve predicted gene structures, and to record textual annotations and protein function. As of December 15, 2009, 1,628 genes (11%) have been manually curated. All annotations, both automatic and manual, may be viewed at a dedicated JGI portal (<http://www.jgi.doe.gov/volvox/>).

I. *Volvox* has longer introns than *Chlamydomonas*

The median intron size in *Volvox* is about twice that of *Chlamydomonas* (358 bp vs. 174 bp; Table 1, Fig. S6). (Mean length and S.D. in *Volvox* are 491 bp and 749 respectively, and 371 bp and 527 in *Chlamydomonas* respectively (Table S7)) This differential accounts for 10.5 Mb of the longer assembly in *Volvox*. 3.5Mb of the *Volvox* introns are made up of repeats, the composition of which reflects the overall repeat class composition of the genome (see above). The length of introns at conserved positions between orthologous exons in *Volvox* vs. *Chlamydomonas* divide into three subpopulations (Fig. S6), each of which has a mean that is significantly different from the others (Welch's t-test, $p < 2.2E-16$). The majority (93%) orthologous introns are >100 bp long and show no size correlation between the two species (Pearson's $r^2 = 0.0044$), though the mean length in *Volvox* (440 bp) is significantly longer than in *Chlamydomonas* (313 bp) (Welch's t-test, $p < 2.2E-16$). A small (3%) subset of introns are short (~60-100 bp) in both species lie near the diagonal (although only weakly correlated, Pearson's correlation coefficient = 0.39) suggesting the existence of a common yet unknown selective mechanism. The third small subset of *Volvox* introns (4%) are around 60-100 bp long but have an uncorrelated length in *Chlamydomonas* (Pearson's $r^2 = -0.0096$) and appear as a horizontal distribution across the bottom of the plot.

J. Pfam protein domain assignments

To assign Pfam domains to proteins in a predicted proteome, we made a set of the longest protein sequence at each locus and ran the HHMPFAM module within InterProScan (S18) with Pfam v20 on these sequences. This algorithm assigns Pfam domains based on the gathering threshold specific to each HMM rather than using the same E-value for every domain.

K. Pfam domain combinations unique to Chlamydomonodales

The last common ancestor of *Volvox* and *Chlamydomonas* is represented by the clade Chlamydomonodales (taxonomy ID 3042) in the NCBI taxonomy (S8). To compare the protein domains found in species inside this clade to those found

outside, we took our Pfam annotations in *Volvox* and *Chlamydomonas* (see above) and added all Pfam domain annotations in Uniprot (ftp://ftp.pir.georgetown.edu/databases/iproclass/; release date 9/3/08) from all other species that are descended from the Chlamydomondales node.

To date, no protein domains unique to the Chlamydomondales have been deposited in the Pfam database. 2,650 domains are found in species within and outside the Chlamydomonodales while 7,690 are only found in species outside this group.

L. Pfam domain combinations specific to *Volvox* or specific to *Chlamydomonas* or both

We counted the number of different pairwise domain combinations in various species (Table S9), considering only unique pairs of protein domain types, regardless of how many times any domain occurs in a protein. In a search for Pfam domain combinations that are present in the volvocine algae (the clade represented by descendants of the last common ancestor of *Volvox* and *Chlamydomonas*), but not in other species, we found only a single domain combination in *Volvox* or *Chlamydomonas* and not other species in uniprot (ftp://ftp.pir.georgetown.edu/databases/iproclass/; release date 9/3/08). After this analysis, the JGI released a genome portal for another species in Chlorophyta, *Chlorella* sp. NC64A (http://genome.jgi-psf.org/ChlNC64A_1/ChlNC64A_1.home.html). The domain combination is found in *Chlorella* too. From this, we conclude that there are no volvocine alga-specific domain combinations.

We also found 199 domain combinations that are present in *Volvox* but not *Chlamydomonas* or other species and, conversely, 122 that are present in *Chlamydomonas* but not *Volvox* or other species. The majority of the gene models in these two sets have no EST support across their lengths and are on short, poorly assembled scaffolds that often include only one WGS read's length of sequence at each end and an internal gap several kb in length, suggesting that the gene models may span more than one genetic locus. This suggests there are few Pfam domain combinations found in one alga and not the other.

M. Construction of protein families

We compared the reference set of 14,520 predicted proteins from *Volvox* and 14,516 predicted proteins from *Chlamydomonas* to each other and to proteins from twenty other organisms spread across the entire tree of life, including animals, plants, fungi, amoebae, chromalveolates and bacteria (Table S10). [In addition to these species, the recently-published predicted proteomes of two *Micromonas* species (S25) were used in the analysis of protein families specific to the Volvocine algae (see below)]. Protein comparisons were performed using WU-BLASTP 2.0MP-WashU [04-May-2006] (S10) with filtering from low-

complexity sequences and simple repeats and Smith-Waterman post-processing. (To determine the cutoff for protein family construction, we manually examined BLASTP alignments at different E-values. We found that a cutoff of E-value $< 1E-10$ included proteins with distinct regions of homology compared to E-values $\geq 1E-10$ that had scattered regions of similarity in the alignments that appeared to be present by chance.) Mutual best hits (E-value $< 1E-10$) between a protein in *Volvox* and a protein in any of the 21 other species including *Chlamydomonas* (as well as mutual best hits between a protein in *Chlamydomonas* and a protein in any of the 21 other species including *Volvox*) were used to establish orthology. Paralogs were added according to empirically-determined criteria that include in-paralogs. In a final step, proteins that were not in families were pledged to a family if their best hit (E-value $< 1E-20$, coverage $> 50\%$) was in a family, another good hit (E-value $< 1E-20$, coverage $> 50\%$) was in the same family, and the family had 50 or fewer proteins in it before pledging. This E-value and coverage cutoffs were determined by choosing a few dozen families and comparing the range of E-values and coverages of proteins within families to those of proteins that had similarity, yet had not been included in the protein families, making them candidates for pledging.

There are 7,612 mutual best hit relationships between *Volvox* and *Chlamydomonas* proteins. These, together with 168 mutual best hits between another species and either *Volvox* or *Chlamydomonas* form the backbone of 7,780 families (with the latter 168 families lacking proteins from either *Volvox* or *Chlamydomonas*). After addition of paralogs 7,293 contain 9,311 (64%) *Volvox* proteins and 7,233 contain 9,189 (64%) *Chlamydomonas* proteins. We found that 3,683 families (containing 3,809 *Volvox* proteins) are also conserved in moss (5,765 proteins) and 3,204 families (containing 3,309 *Volvox* proteins) are also conserved in *Arabidopsis* (4,141 proteins).

Notably, 10 of these families have a single member in *Chlamydomonas* and more than five members in *Volvox* whereas only two families have a single *Volvox* member and more than five *Chlamydomonas* members (Table S11). There are only 80 families (1.1%) with over 5 proteins from *Chlamydomonas* and/or *Volvox*. 295 families contain a single *Volvox* protein and 2-5 *Chlamydomonas* proteins, while 282 families contain a single *Chlamydomonas* protein and 2-5 *Volvox* proteins.

N. *Volvox*-specific genes

We were interested in identifying how many novel protein coding genes had appeared in the *Volvox* lineage since divergence from *Chlamydomonas*, since these proteins could encode *Volvox*-specific functions. From a starting set of 5,209 *Volvox* proteins that had not been placed into a protein family (see above), we identified 142 putative potentially *Volvox*-specific proteins based on the following three criteria: these proteins had no TBLASTN hit to the

Chlamydomonas genome assembly (E-value < 1E-10); at least one splice site supported by EST evidence and no BLASTP hit (E-value < 1E-10) to any protein from any of the proteomes we had used to make the protein families (Table S10 and see above).

We found 84 of the 142 proteins had BLASTP homology (E-value < 1E-10) to at least one other protein in the set, suggesting they are part of a protein family; the remaining 58 were singletons (Table S12). The quality of each of the 142 putative *Volvox*-specific gene models was inspected manually on the JGI genome browser at <http://www.jgi.doe.gov/volvox>. Many of these models were short and/or based solely on *ab initio* gene modelling and/or had no EST evidence or conflicted with EST evidence. Nonetheless, 25 gene models were completely consistent with EST evidence, and a further 11 gene models have partial EST support (Table S12). When we searched these 36 gene models against the protein sequences from the two *Micromonas* genomes (S25) using BLASTP (E-value < 1E-5) we found no detectable homology.

Intriguingly, none of the known *Volvox* developmental regulators was in this set of *Volvox*-specific proteins. Our analyses suggest that there are a small number of *Volvox*-specific proteins, despite substantial differences in developmental complexity between *Volvox* and *Chlamydomonas*.

O. *Chlamydomonas*-specific genes

In a parallel analysis to that performed for *Volvox*-specific genes, we identified 757 putative *Chlamydomonas*-specific genes from a starting set of 5,327 proteins that we were not able to place in a protein family. The larger number of *Chlamydomonas*-specific proteins compared to the number of *Volvox*-specific proteins may in part be due to deeper EST coverage in *Chlamydomonas*.

We found 238 of the 757 proteins had BLASTP homology (E-value < 1E-10) to at least one other protein in the set, suggesting they belong to a *Chlamydomonas*-specific protein family; the remaining 519 were singletons (Table S13). We chose a random sample of 50 putative *Chlamydomonas*-specific gene models from each of the above classes and examined the gene models manually at <http://genome.jgi-psf.org/Chlre3/Chlre3.home.html> and hence estimate that 32% and 60% of the models respectively are completely consistent with EST data (Table S13). We extrapolate this analysis to suggest that *Chlamydomonas* may have up to 400 novel proteins.

P. Volvocine algae-specific protein families

We investigated three classes of proteins that are only found in volvocine algae (defined as the group of organisms that includes *Volvox* and *Chlamydomonas*, as well as other species, such as *Gonium*, *Pandorina*, *Eudorina* and *Pleodorina* for which genome sequences are not yet available (Fig. S2) and see below). We

discuss the results in this section and the next two sections, where presence or absence of a protein was based on the protein families described above. The first class of proteins is those found in both *Volvox* and *Chlamydomonas* but not other organisms. The second class consists of proteins that are only found in *Volvox*, and the third class consists of proteins that are only found in *Chlamydomonas*. These last two classes of proteins (together with various changes in regulation) might be associated with specific developmental and ecological adaptations in each species (see below).

We found 1,835 volvocine-specific protein families out of the total of 7,780 (Fig. 2B). To perform this analysis, we included data from the genomes of two *Micromonas* species that have been published recently (S25). These prasinophytes are substantially less reduced than the related *Ostreococcus* species that we had used in constructing protein families. We re-examined the 2,018 volvocine-specific families from our protein families in the light of this new data. We compared all *Volvox* and *Chlamydomonas* proteins in these families to all proteins in the predicted proteomes of *Micromonas pusilla* CCMP1545 v2.0 (<http://genome.jgi-psf.org/MicpuC2/MicpuC2.home.html>) and *Micromonas pusilla* sp. RCC299 v3.0 (<http://genome.jgi-psf.org/MicpuN3/MicpuN3.home.html>) using WU-BLASTP (S10) (E-value < 1E-10). We removed 183 families containing a *Volvox* and/or *Chlamydomonas* protein that had a mutual best blast hit to a *Micromonas* protein. This left 1,835 volvocine-specific families. (Fig. 2B,D). Although these families have not been extensively characterized, they are expected to function in processes that are specific to volvocine algae and indeed, they include families of extracellular matrix proteins that participate in formation of the cell wall and ECM (Fig. 3A, S8).

Q. Analysis of Transcription Associated Proteins

Transcription associated proteins (TAPs) include transcription factors (TFs, proteins that bind to *cis*-regulatory elements enhancing or repressing gene transcription) and transcriptional regulators (TRs, proteins with indirect regulatory functions, such as the assembly of the RNA polymerase II complex, functioning as scaffold proteins in enhancer/repressor complexes or controlling chromatin structure by modifying histones or the DNA methylation).

To identify the TAPs in *Volvox* and *Chlamydomonas*, we combined three sets of TAP classification rules for plants, PlantTFDB (S26), PlnTFDB (S27) and PlanTAPDB (S28), and expanded them to yield a set of classification rules for 111 families. Conflicts between the initial three sources were manually evaluated and resolved based on an analysis of the scientific literature. The resulting set was then expanded by adding recently defined families or subfamilies from published sources. The rule set for each family consists of at least one entry defining a "should" rule, i.e. a mandatory domain for that particular family. Additional

entries may define further "should" or "should not" (forbidden) domains. All domains relevant for classifying the TAPs were represented by a full length, global (termed "ls") HMM. If available, the HMMs were retrieved directly from the 'PFAM_ls' database (S29). For the remaining domains, HMMs were custom-made using multiple sequence alignments (MSAs) to identify the conserved domain(s) of interest. The MSAs used for creating the custom HMMs were downloaded from PlnTFDB (S30). For domains not represented in this database, MSAs were created as follows. BLAST searches with a protein query containing the respective domain yielded homologous hits defined by having at least 30% sequence identity with the query over a minimum length of 80 amino acids. Those hits were aligned using MAFFT (S31) and manually curated using Jalview (S32). The conserved domain of interest was extracted and the HMM calculated with HMMER 2.0 (<http://hmmer.janelia.org/>) using 'hmmbuild' with the default parameters to generate ls HMMs and subsequently 'hmmcalibrate' with the option '--seed 0' which sets the random starting seed to a constant value and hence obtains reproducible results during the calibration process.

Gathering cutoff (GA) values were defined for each custom HMM. The GA was set as the lowest score of a domain-containing protein (true positive) after a 'hmmpfam' search (using an E-value cutoff of 1E-5) against the full proteome sets of several different species and considering the alignments of all hits. In order to avoid sampling bias, only fully sequenced genomes were used in this study. For each organism, the complete set of proteins derived by conceptual translation of the nuclear gene models (using the filtered/selected model per locus) was combined with the proteins encoded by the respective mitochondrial and plastid genome, if available. All proteins can be unambiguously identified via their fasta id. We used a unique five letter code for each organism followed by "mt" (mitochondrial) or "pt" (plastid), if applicable, and the accession number of the gene model.

Using all proteins of the investigated organisms as query, 'hmmpfam' searches were performed against an HMM library containing all 129 domains necessary for the TAP classification. The GA was used during this procedure to minimize the number of false positive hits, with GA values either provided with the Pfam HMMs or defined as described above. The classification rules were subsequently applied to all proteins for which at least one significant domain hit was found. In cases where the domain composition of a protein matched more than one classification rule, the 'should' rule with the highest score determined the family into which the protein was categorized.

Highly similar domains which are often found in the same or overlapping regions of a protein were treated in similar fashion, i.e., the domain with the lowest E-value/highest score was used for the subsequent classification. This procedure was necessary for four sets of domains, namely i) Myb_DNA-binding and G2-like_Domain, ii) NF-YB, NF-YC and CCAAT-Dr1_Domain, iii) PHD and Alfin-

like and iv) GATA and zf-Dof. In addition, a Boolean OR rule was applied to three families. In these cases one out of two domains was found to be necessary and sufficient for a protein to be classified into the corresponding family. This rule was applied to the bZIP, HD-Zip and GARP_ARR-B families. Whenever the presence of a combination of domains led to more than one possible family classification, TF was favored over TR or PT (putative TAPs). This situation was encountered in 14 cases.

In *Volvox*, the proportion of all proteins that are transcription factors is 347/14,520; in *Chlamydomonas* it is 297/14,516 (Table S15). This proportion is not significantly higher ($p=0.02831$, one-tailed Fisher Exact test) in *Volvox* compared to *Chlamydomonas*. A scatter plot of the number of *Volvox* vs. *Chlamydomonas* proteins in each TAP family (Fig. S7) shows that most families lie on or near the diagonal, with the larger families showing slight over-representation of *Volvox* proteins.

R. Annotation of genes associated with developmental biological processes in *Volvox*

Membrane trafficking proteins

We started with a set of SNARE and Rab GTPase proteins from *Chlamydomonas* (S14, 33) and searched for appropriate gene models in homologous regions in the *Volvox* genome using TBLASTN (E-value < 10). Reciprocal searches were conducted to identify the mutual best hit pairs between the two species. The NCBI nr protein database (S8) was also queried with each protein from *Volvox* to identify the best hit in another species such as human, *Arabidopsis* and yeast (S34) which were then used as the query protein in searches against the *Volvox* and *Chlamydomonas* genomes. Finally, to assign a family name to each protein, we performed phylogenetic analysis for Rab proteins (aligning proteins and building 1,000 bootstrap neighbor-joining trees using CLUSTAL X 1.82 (S35)) and Syp proteins (aligning proteins with CLUSTAL X 1.82 (S35) and MUSCLE (S36), and building 100 bootstrap maximum parsimony trees with PAUP* 4.0 beta 10 (S37)) using *Volvox* and *Chlamydomonas* proteins and *Arabidopsis* and human homologs found by BLAST searches at the nr database at GenBank (S8).

Cell cycle proteins

We started with a set of cell cycle proteins from *Chlamydomonas* (S38) and searched for homologs in *Volvox* using BLASTP and TBLASTN (E-value < 10). Reciprocal searches were conducted to identify mutual best hit pairs between the two species. The NCBI nr protein database (S8) was also queried with each predicted cell cycle protein from *Volvox* and *Chlamydomonas* to identify the best hit in another species, which was then used as the query protein in searches against the *Volvox* and *Chlamydomonas* genomes and predicted proteomes. This process was iterated until all significant BLAST hits between cell cycle proteins

and gene models in *Chlamydomonas* and *Volvox* had been identified. For each cell cycle gene model identified in *Volvox*, flanking genes were used to identify synteny with the putative orthologous model in *Chlamydomonas*. In all cases the synteny was in agreement with orthology assignments based on mutual best hits. In addition, an identical approach was used to identify *Volvox* and *Chlamydomonas* orthologs, this time starting with all *Volvox* proteins with PFAM or KOG domain assignments specific to cell cycle regulation.

Cytoskeletal proteins

We searched the GenBank nr database (S8) for members of known cytoskeletal protein families (S39), and used sequences identified from *Arabidopsis* (or *Drosophila* when *Arabidopsis* hits were not found) as queries in TBLASTN searches (E-value < 0.01) against the *Volvox* and *Chlamydomonas* genome assemblies at the *Volvox* or *Chlamydomonas* genome portal at the JGI. We assumed proteins without a hit were not encoded in the algal genome. The best gene model from the hit results was chosen, based on E-value, EST evidence and homology to the other algal genome and generally gave best hit E-values < 1E-7 when queried back against GenBank by BLASTP. Each protein model obtained in this way was next used as query in a second TBLASTN (E-value < 1E-5) against both algal genomes to identify additional homologs. This process was repeated until all members of the family were identified. Orthology between *Volvox* and *Chlamydomonas* proteins was inferred when the candidates were mutual best hits in TBLASTN searches and the Vista track at the JGI browser showed significant conservation at the DNA level.

Cell wall and extracellular matrix proteins

We started with a set of known extracellular proteins/ECM proteins /cell wall proteins from *Volvox* (S40, 41).

We made TBLASTN searches (E-value < 1E-7) with the protein sequences against both, the *Volvox* and *Chlamydomonas* genomes. All hits were searched reciprocally against the other algal genome, also using TBLASTN.

Whenever TBLASTN hits corresponded to an existing gene model, the model was used, or the model was edited or a new model was generated using the JGI portal.

Phylogenetic analyses

The following describes the phylogenetic analyses used to generate the trees in Fig. 3. Homologous protein sequences were aligned with MUSCLE (S36). Poorly-aligning end regions were trimmed and the sequences were realigned. The process was repeated until no further improvements could be made. Positions with gaps were removed prior to construction of phylogenies. ProtTest (S42) was used to select the best model of protein evolution for each set of proteins. Maximum likelihood trees were constructed using PhyML 3.0 (S43, 44) under

the following parameters: 100 bootstrap replicates; four-category gamma distribution; proportion of variable sites estimated from the data.

2) SUPPORTING TEXT

A. Volvocine algae as a model for the evolution of multicellularity

In addition to its strengths as a developmental-genetic model, *Volvox*, together with its relatives in the “volvocine lineage” (Fig. S2), provides an unrivalled opportunity to explore the details of a pathway by which multicellular organisms with differentiated cell types evolved from a unicellular ancestor – one of the most complex and interesting steps in the evolution of higher organisms (S45). Formation of a multicellular body of predictable shape and size has usually required the invention of novel morphogenetic mechanisms, while differentiation of two or more distinct cell types within such a body has required elaboration of novel spatial patterns of gene expression. This is likely true in *Volvox* too. Multicellularity has evolved not just once but repeatedly and independently in a highly diverse array of taxa (S46-48). However, in most cases the transition to multicellularity has occurred so long ago (more than 500 MYA in many cases (S47, 49, 50) that most details of the molecular genetic changes leading to multicellularity have diverged so much they can no longer be studied.

It has long been suggested, however, that the volvocine algae provide an interesting exception to the preceding generalization. The volvocine lineage comprises several genera of green flagellates that can be arranged in a conceptual series according to increasing complexity (Fig. S2) – *Chlamydomonas*, *Gonium*, *Pandorina*, *Eudorina*, *Pleodorina*, *Volvox* – within which there are progressive increases in cell number, size of adult organisms, volume of ECM per cell, and the tendency to produce sterile, terminally differentiated somatic cells. Recent molecular-phylogenetic analyses not only indicate that these algae constitute a coherent, monophyletic group that began its radiation within the last ~200 MYA (S51) (S52), but also that the sequence indicated above serves as a reasonable first approximation of the historical sequence in which members of the group evolved (S53). Furthermore the allure of volvocine algae as an evolutionary model system is significantly enhanced by the finding that the kind of germ-soma division of labor that has traditionally earned an alga membership in the genus *Volvox* has arisen independently on at least four separate branches of the volvocine family tree (S54)

Molecular-genetic studies of *Volvox* embryogenesis have already indicated that different aspects of the evolution of *Volvox* from a *Chlamydomonas*-like ancestor have involved qualitatively different amounts of genetic change. For example, the *glsA* gene (whose product is required for the asymmetric divisions that set apart the germ and somatic cell lineages of *Volvox* embryos) (S55) obviously was adopted for this novel function with no significant changes, because the orthologous *GAR1* gene of *Chlamydomonas* is fully capable of substituting for it (S56), even though there is no known asymmetric division in the *Chlamydomonas* life cycle. Similarly, the *invA* gene (whose product is a kinesin

that the *Volvox* embryo requires for inversion at the end of embryogenesis) can be replaced by its *Chlamydomonas* ortholog, *IAR1* (S57), indicating that this gene was also adopted to play an entirely novel morphogenetic role without any significant evolutionary modification of the protein that it encodes. In marked contrast, *Chlamydomonas* lacks any recognizable ortholog of the *regA* gene of *Volvox* that plays a central role in differentiation and programmed death of somatic cells (apparently by repressing chloroplast biogenesis; (S58) (S59)): *regA* encodes an entirely novel combination of pre-existing and new protein domains, of which only the sequence of the presumed DNA-binding domain can be traced back to its Chlamydomonad ancestry (S60).

The attractiveness of *Volvox* as a developmental and evolutionary model is enhanced by the availability of several important molecular tools, including a variety of selectable markers (S61-64), a transposon-tagging system (S65, 66), a nuclear transformation system (S67), and a reporter gene (S68).

B. The *Volvox* vegetative life cycle

Volvox has two cell types: ~2,000 small, biflagellate *Chlamydomonas*-like somatic cells that are embedded in the surface of a transparent sphere of glycoprotein-rich extracellular matrix (ECM), and ~16 large reproductive cells (termed gonidia) that lie just below the somatic cell monolayer (S69). Each gonidium grows, divides and undergoes morphogenesis to produce the next generation (Fig. S1B). Asymmetric cell divisions during embryogenesis determine the germ-line precursors. Following cleavage, the embryo turns inside-out in a process called inversion; inverted juveniles expand by the deposition of ECM, and finally hatch out of the mother colony to complete the life cycle.

C. The *Volvox* sexual cycle

Sexual development in *Volvox* and *Chlamydomonas* is controlled by a large, multigenic, haploid mating locus (*MT*) that segregates as a single Mendelian trait. *MT* occupies the same chromosome in both species, but is five times larger in *Volvox* relative to *Chlamydomonas* (S70). Both sexes of *Volvox* have the same vegetative developmental cycle that is described in the preceding section. However, in response to a diffusible sex inducer protein *Volvox* males and females undergo modified developmental programs to produce sperm packets and eggs, respectively (S71). This developmental response to sex inducer involves changes in the timing of asymmetric cell division, altered gametic gene expression (S72, 73), and male germ cell divisions into sperm packets.

D. The *Volvox* ECM

The *Volvox* ECM comprises up to 99% of the spheroid volume (reached in the adult shortly before release of daughter spheroids) and provides a highly organized substrate that compartmentalizes its interior space (Fig. S3). It is likely to be involved in intercellular signaling and nutrient transport (S40).

Evolutionarily, the *Volvox* ECM can be understood as a massive elaboration of the cell wall of *Chlamydomonas*. In both organisms the cell wall and ECM are composed of hydroxyproline-rich glycoproteins (HRGPs) that form rod-like structures and which often have additional globular domains at each end (S74). In *Volvox*, individual pherophorin subtypes are associated with distinct regions of the ECM, and each subtype is likely to be involved in the assembly and/or specific function of these ECM subdomains (also referred to as ECM subzones) (S74).

E. Environmental adaptations of *Volvox* and *Chlamydomonas*

Volvox and *Chlamydomonas* are cosmopolitan species and occupy overlapping habitats (S75). *Chlamydomonas* can proliferate in more transient bodies of water than *Volvox*, thanks to its faster generation time and smaller size. While *Chlamydomonas* is often portrayed as a soil alga, it is usually collected from soil in the form of environmentally resistant and dormant zygospores which can travel long distances and last for years under unfavorable conditions (S75, 76). Thus, the places where *Chlamydomonas* is collected provide only a partial indication of the environment to which it was adapted and in which it proliferates. On the other hand, *Volvox* and other multicellular volvocine algae are generally collected as live specimens from permanent or semi-permanent bodies of water; but such collection sites are biased against transient and unreliable locations. Thus, the specific environmental adaptations that may have arisen in the two species have not been systematically examined.

3) SUPPLEMENTAL FIGURES

Fig. S1: *Volvox* phylogeny, morphology and development.

(A) The phylogenetic position of *Volvox* and *Chlamydomonas* (within Chlorophyceae, green) is shown in an unrooted schematic cladogram of the eukaryotic tree of life (Sfrom 47); open and filled triangles denote clades consisting of solely unicellular lineages, and clades comprising both unicellular and multicellular lineages, respectively. (B) The asexual life cycle of *Volvox* with photomicrographs, taken as described in (S66), of a newly-hatched adult (top left, bar = 200 μ m) and of an adult *Volvox* (lower right, bar = 500 μ m) as well as scanning electron micrographs of an embryo after the first asymmetric cell division at cleavage cycle 6 (top right inset) and of a post-cleavage embryo during inversion (middle right inset). Each micrograph is placed near its corresponding developmental stage in the schematic diagram.

Fig. S1

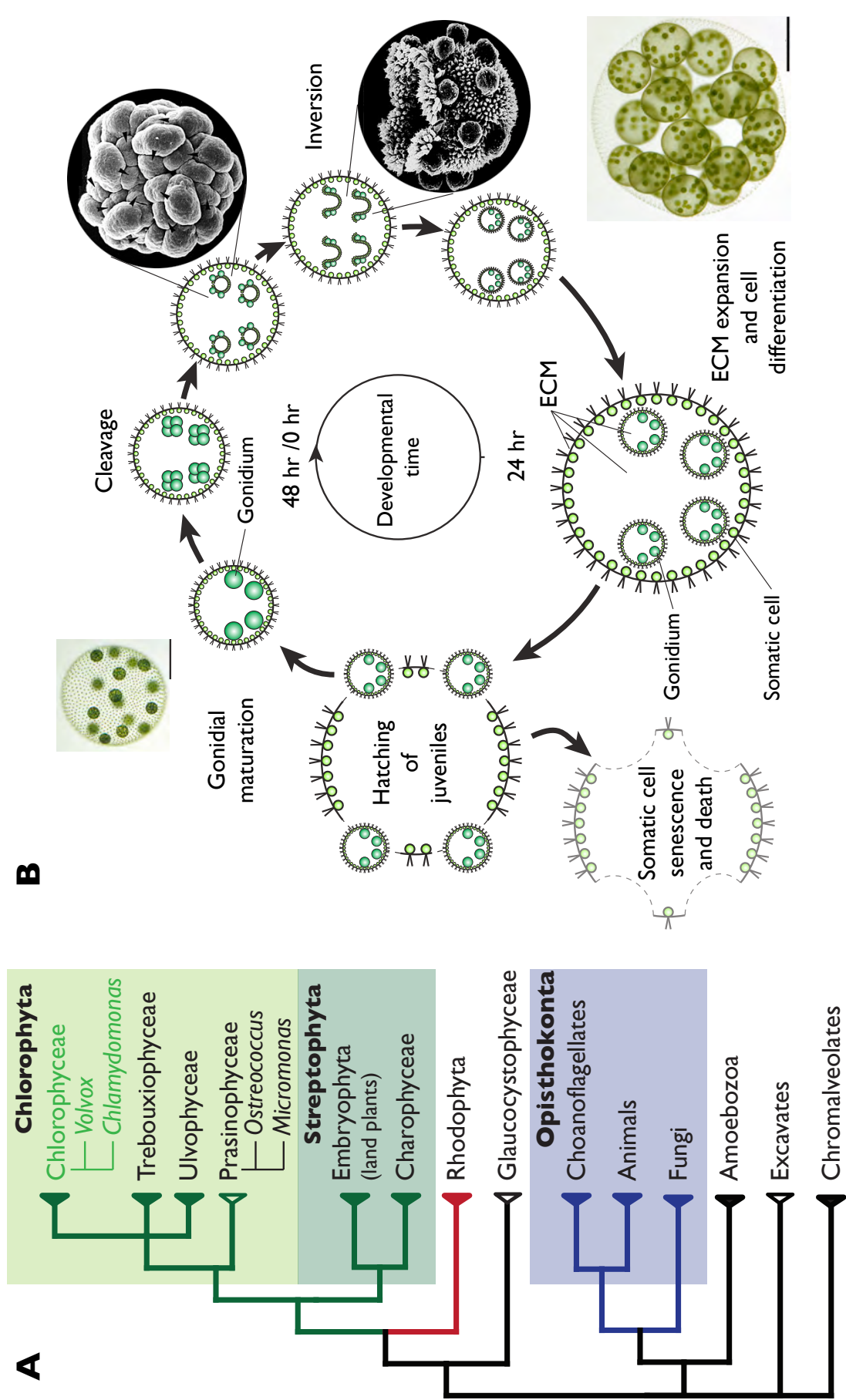


Fig. S2: The algae of the volvocine lineage

The volvocine algae comprise dozens of species that range in complexity from *Chlamydomonas* through colonial forms that have evolved different types of developmental traits. Photomicrographs of representative species from key genera are arranged along the top of the chart. The presence of the developmental traits listed along the left side is indicated in the grid by a 'X'. The photomicrographs were taken as described in (S66). Strains used are as follows: *Chlamydomonas reinhardtii* strain c-239+ (S77); *Gonium pectorale* strain kaneko3 (S78); *Pandorina morum* strain NIES-877; *Eudorina elegans* strain NIES-721; *Pleodorina starii* (female) (S79)

Fig. S2

Developmental trait(s)	<i>Chlamydomonas reinhardtii</i>	<i>Gonium pectorale</i>	<i>Pandorina morum</i>	<i>Eudorina elegans</i>	<i>Pleodorina starnii</i>	<i>Volvox carteri</i>
Unicellular	X					
Cell sheets		X				
Partial inversion						
Spherical colonies			X		X	X
Full inversion					X	X
Incomplete cytokinesis					X	X
Expansion of ECM					X	X
Anisogamy					X	X
Partial division of labor					X	
Complete division of labor						X
Asymmetric cell division						
Bifurcated cell division program						

Fig. S3: Schematic diagram of ECM in *Volvox*

In this schematic cross-section of a *Volvox* adult (redrawn from (S71, 75, 80)), the elaboration of the ECM into deep, cellular and boundary and flagellar zones is shown, with the three subzones of the cellular and boundary zones surrounding a single zoomed in somatic cell. Fibrous cellular zone 1 is attached to the somatic cell body plasmalemma, cellular zone 2 is relatively amorphous; fibrous cellular zone 3 forms compartments around the somatic cells. The boundary zone is continuous except where interrupted by flagella, the dense fibrous boundary zones 1 and 3 flank the tripartite boundary zone 2. Deep zone 1 is an band of filaments and surrounds the amorphous deep zone 2 (S75).

Fig. S3

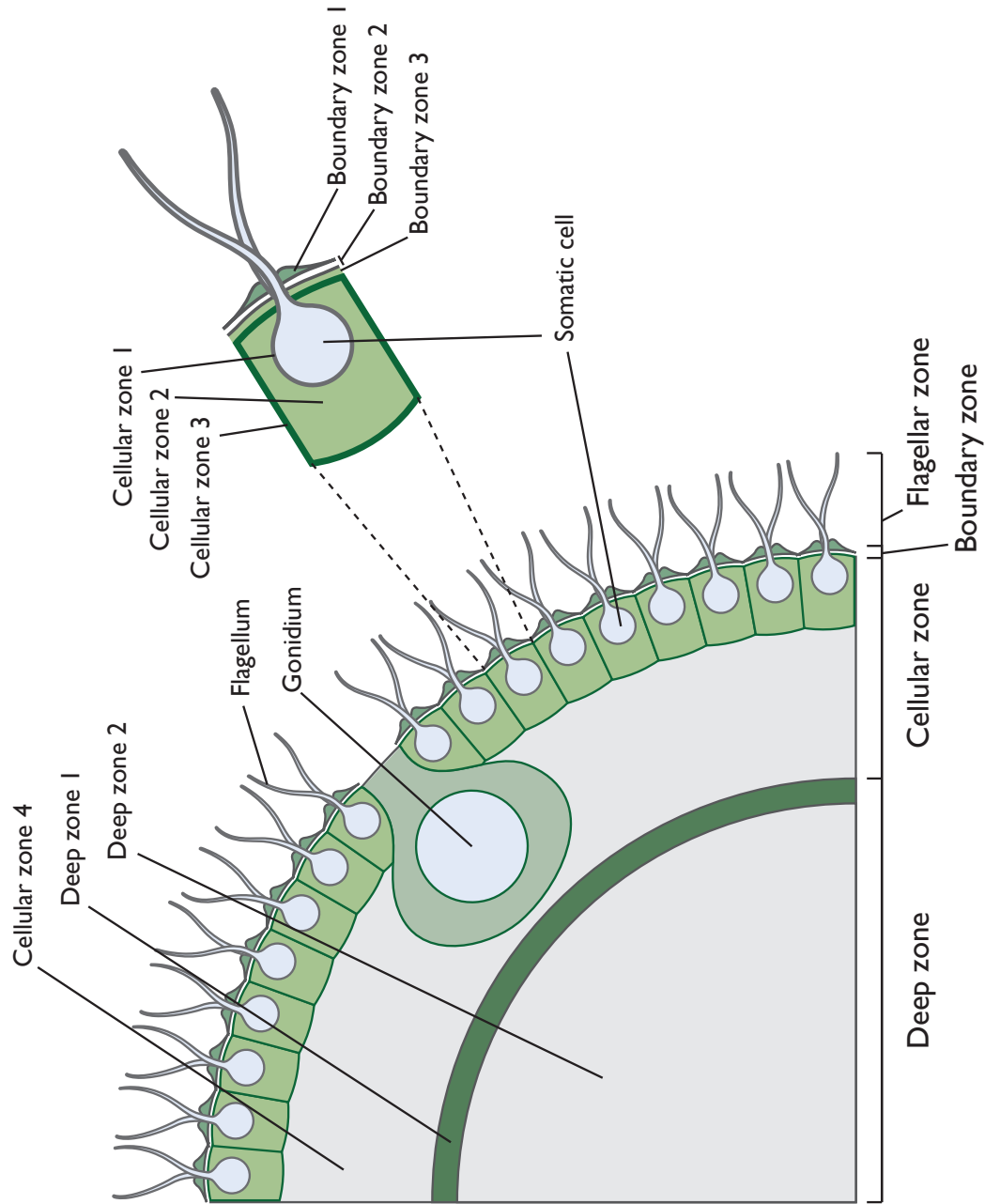
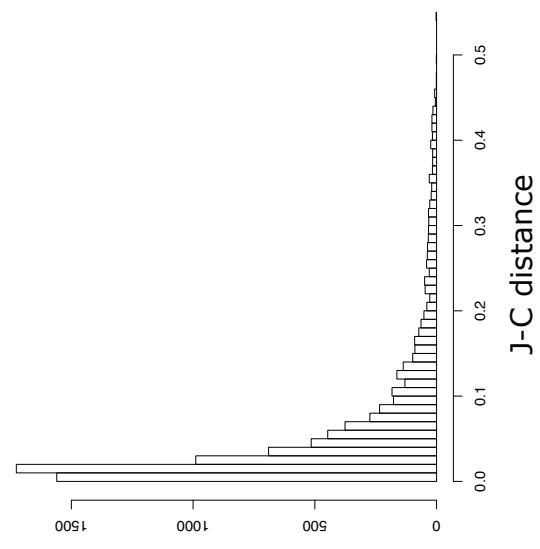


Fig. S4: Histograms of Jukes-Cantor distance between repeats

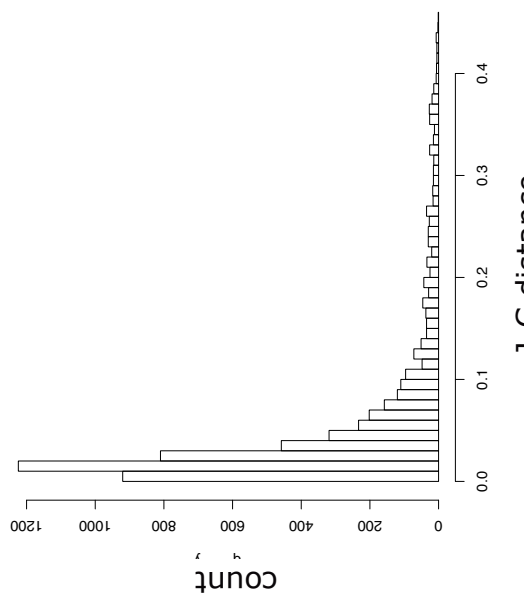
Histograms plot the distribution of sequence divergence (as measured by Jukes-Cantor distance) between repeats within *Volvox* (top row, A-C) and *Chlamydomonas* (bottom row, D-F). They show the distances between all repeats identified by Repeat Scout (A,D), Copia elements only (B,E) and Gypsy elements only (C,F).

Fig. S4

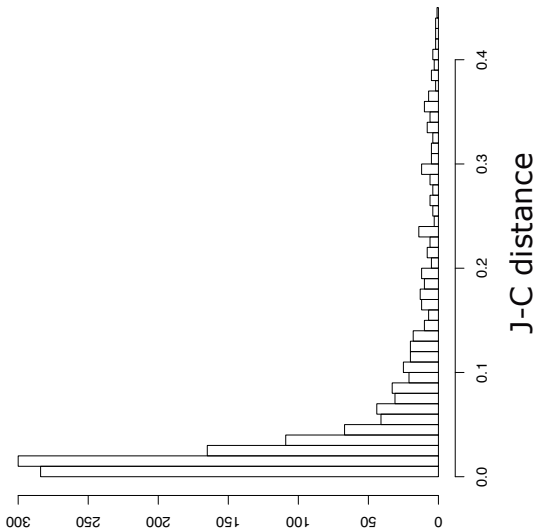
B



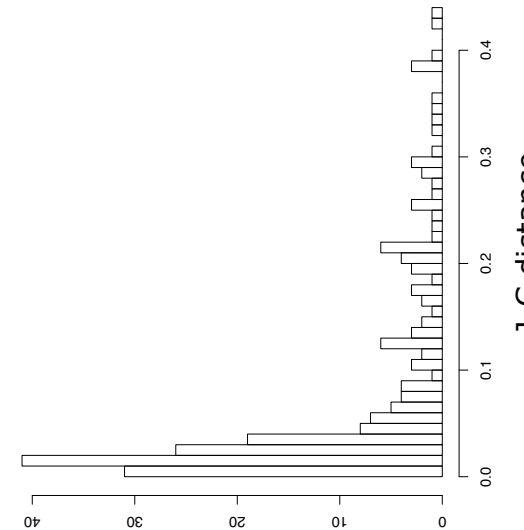
D



C



F



E

Fig. S5: Synteny dotplot between *Volvox* and *Chlamydomonas* genomes

Conserved gene order plots for (A) *Volvox*-*Chlamydomonas* and (B) human-chicken, showing locations of syntenic orthologs (max 2 intervening genes, segment size 2 or more genes). Syntenic genes lie along the two axes. These are arbitrarily numbered as follows: syntenically orthologs are numbered along scaffolds (*Volvox*) or chromosomes (*Chlamydomonas* v4 assembly, human and chicken) from largest to smallest, arbitrarily starting at 1 for the x-axes and 100,000 for the y-axes. unmap, chicken scaffolds that have not been mapped to a chromosome.

Fig. S5

B

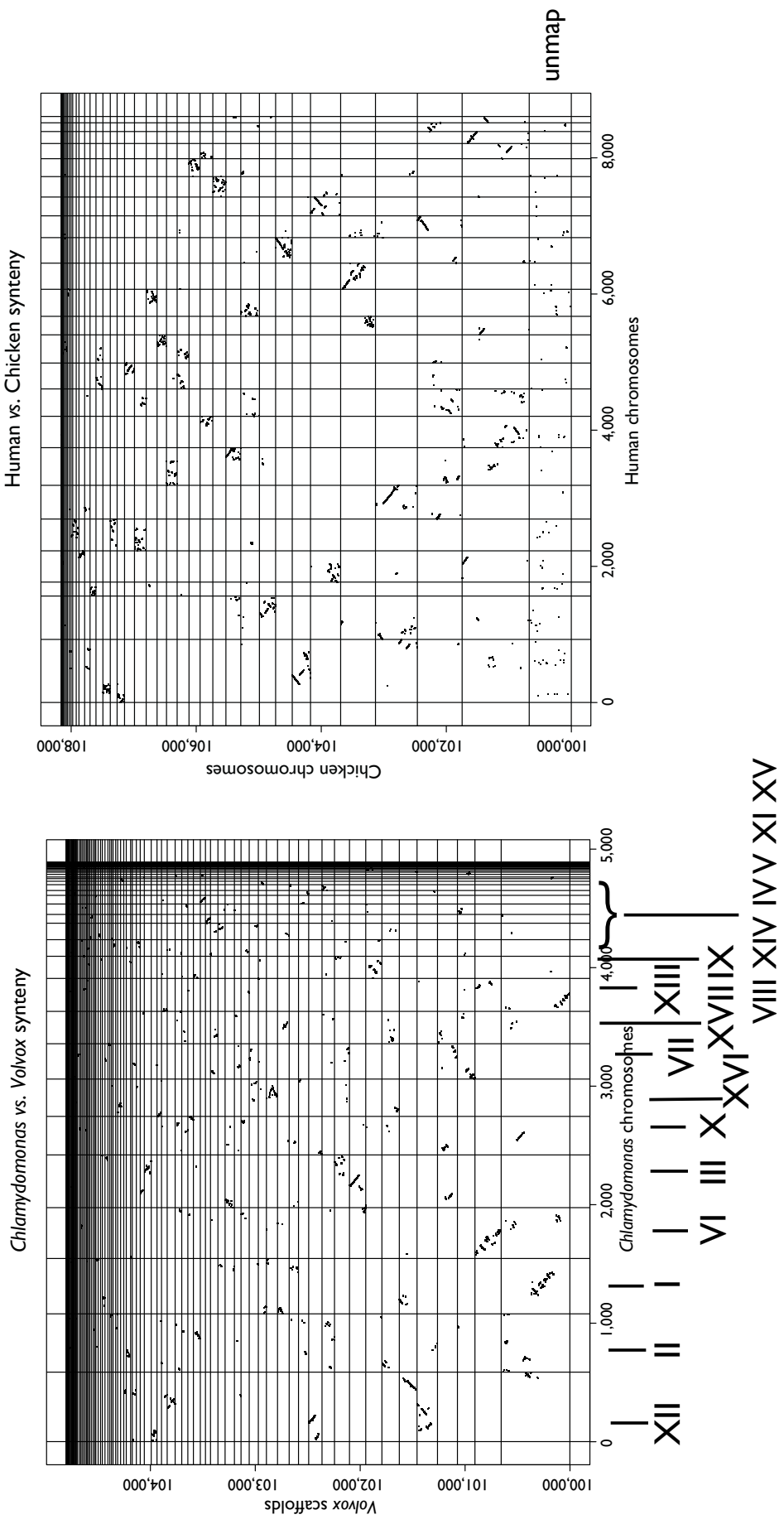


Fig. S6: Intron lengths in *Volvox* and *Chlamydomonas*

The length of introns at conserved positions between orthologous exons in *Volvox* vs. *Chlamydomonas* is shown in a scatter plot (see above). Three subpopulations are evident (boxes). The majority (93%) orthologous introns are >100 nt long, longer in *Volvox* and show no size correlation between the two species. A small (3%) subset of introns are short (≤ 100 nt) in both species and when plotted, lie near the diagonal meaning that they have similar sizes in the two species. Finally, a third small subset of *Volvox* introns (4%) are around 60-100 nt long but vary over a wide size range in *Chlamydomonas* and appear as a faint horizontal smear across the bottom of the plot.

Fig. S6

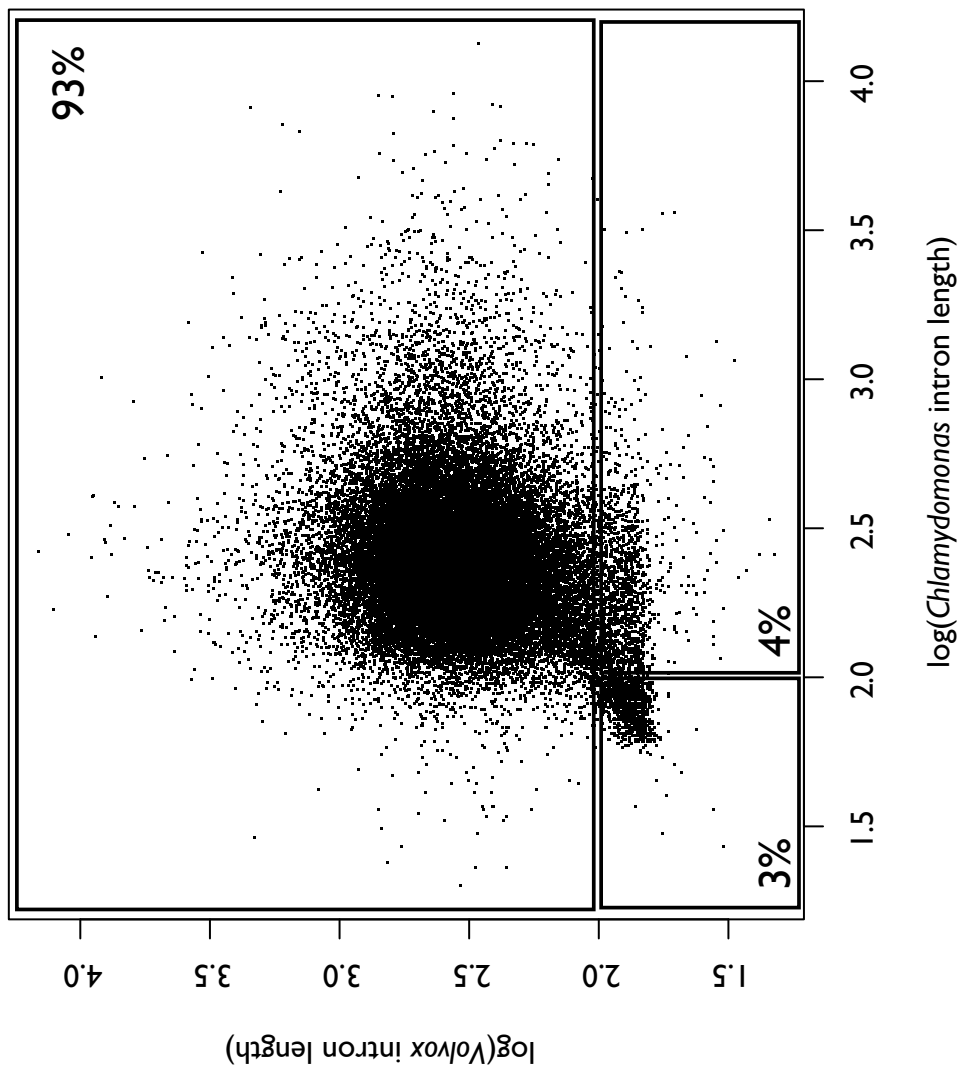


Fig. S7: Scatter plot of family size in transcription associated proteins

The number of *Volvox* proteins in a transcription-associated protein family is plotted against the number of *Chlamydomonas* proteins in the same family. The diagonal line marks the positions of families with equal numbers of proteins from each species. The names of families with more than five members from each species are indicated.

Fig. S7

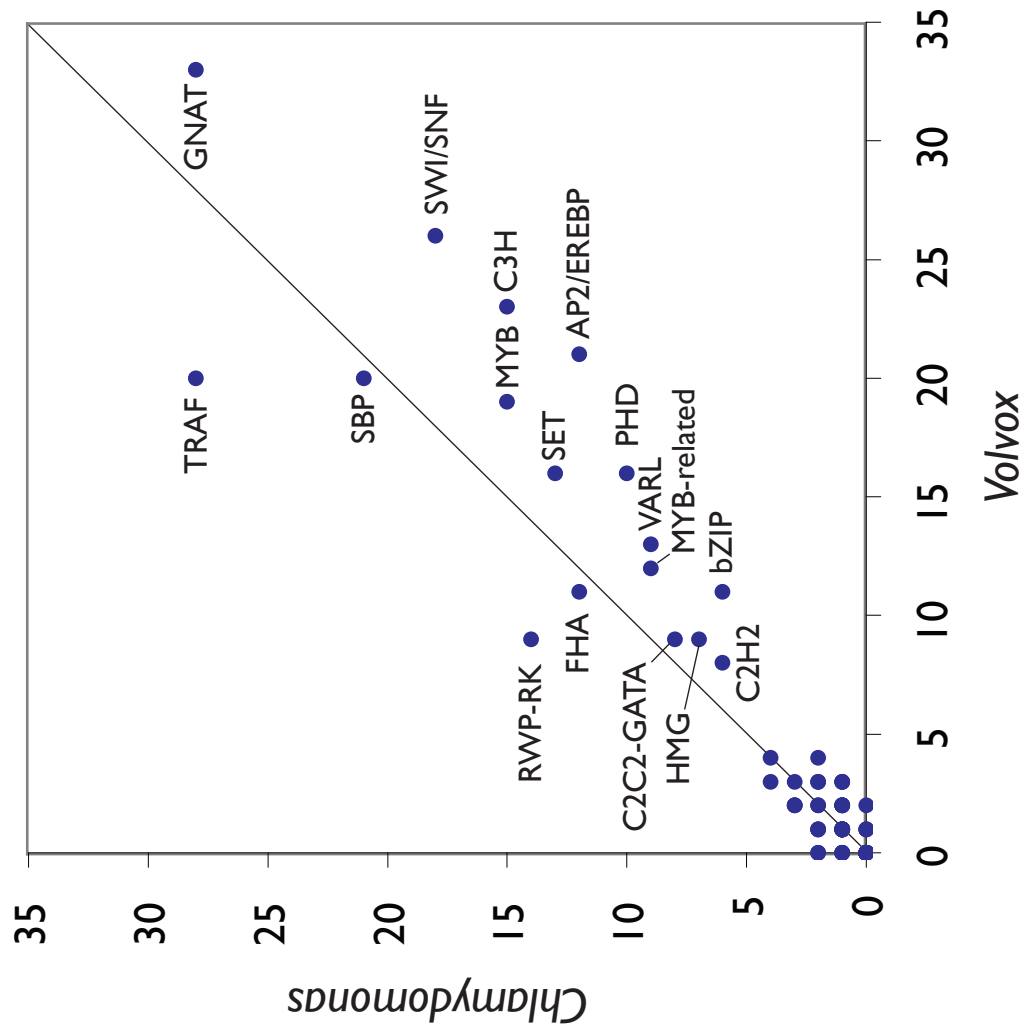
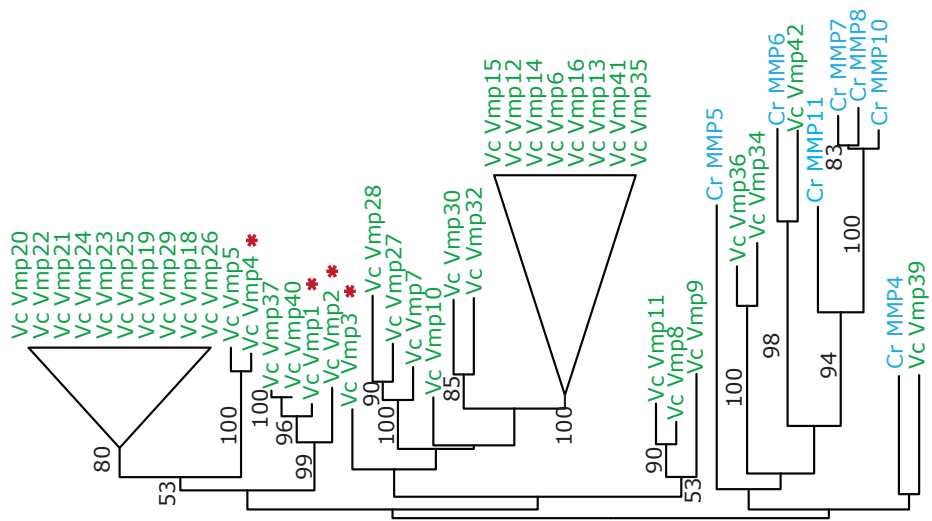


Fig. S8: Diversification of *Volvox* matrix metalloprotease family.

Unrooted maximum likelihood tree of *Volvox* matrix metalloproteases. Protein sequences are from *Volvox* (Vc; green) and *Chlamydomonas* (Cr; blue).

Incomplete gene models were not included ; *Volvox*-specific clades with poorly-resolved branches are collapsed into triangles; bootstrap support $\geq 50\%$ is indicated on branches. Red asterisks indicate proteins whose mRNA levels are up-regulated by sex inducer.

Fig. S8



4) SUPPLEMENTAL TABLES

Table S1: Summary of repeats in *Volvox* and *Chlamydomonas* genomes

The extent (and percentage in parentheses) of the *Volvox* and *Chlamydomonas* genomes that are masked by different classes of repeat family/subfamily and simple repeats are shown. Repeat masking was performed with RepeatMasker and the custom library that we had built for the genome.

Repeat family/subfamily	<i>Volvox</i> assembly	<i>Chlamydomonas</i> assembly
SINEs	298,781 (0.22%)	125,738 (0.11%)
LINEs	2,681,727 (1.95%)	4,544,976 (3.84%)
LTR elements	5,067,964 (3.68%)	890,315 (0.75%)
LTR/Copia	218,136	89,130
LTR/Gypsy	675,620	403,108
DNA elements	1,861,025 (1.35%)	2,003,374 (1.69%)
Jordan	152,065	0
Unclassified	18,267,323 (13.25%)	7,206,766 (6.10%)
Total Interspersed Repeats	28,176,820 (20.44%)	14,771,169 (12.50%)
Satellites	145,736 (0.11%)	489,348 (0.41%)
Simple Repeats	4,561,091 (3.31%)	6,184,379 (5.23%)
Low Complexity	1,246,389 (0.90%)	1,799,865 (1.52%)
Total non-Interspersed Repeats	5,953,216 (4.32%)	8,473,592 (7.17%)
Total Repeats	34,130,036 (24.76%)	23,244,761 (19.66%)

Table S2: Genome evolution in green algae, animals, plants and diatoms

We compare neutral nucleotide substitutions (4DTV), species divergence time, genome rearrangements and protein evolution (mutual best hits) for selected species pairs. N.D. not determined because at least three whole genome duplications since speciation prevented clear assignment of orthologs.

Species pair	Corrected 4DTV	Time since divergence (Myr)	Neighbor rearrangements (%)	Median distance between rearrangements in genome 1 / genome 2 (kb)	Similarity between mutual best BLAST hits (%)
<i>Volvox/Chlamydomonas</i> (green algae)	0.71	~ 220 (S51)	34	6 / 6	73.8
human/chicken (vertebrates)	0.57	~310 (S81)	15	113 / 40	75.9
human/frog (vertebrates)	0.80	~350 (S82)	14	83 / 49	71.8
<i>Arabidopsis/Populus</i> (angiosperms)	0.68	~110 (S83)	N.D.	N.D.	72.0
<i>Thalassiosira/Phaeodactylum</i> (diatoms)	1.94	~90 (S84)	45	2 / 2	54.9

Table S3: Counts of filtered genes that were used to build syntenic blocks

The numbers of genes in the table correspond to syntenic orthologs after tandem duplicates and high-copy gene were removed.

Species	Filtered genes
Human	8,612
Chicken	8,159
Frog	8,158
<i>Chlamydomonas</i>	4,890
<i>Volvox</i>	4,804

Table S4: Counts of *Volvox* and *Chlamydomonas* genes making up syntenic blocks with selected numbers of intervening genes allowed for real and scrambled gene order

This table shows the number of syntenic orthologs that are part of syntenic blocks that were generated when a range of zero to four intervening genes were allowed between syntenic orthologs for both the real gene order, and randomized gene order.

Maximum no. intervening genes	Real gene order	Scrambled gene order
0	2,839	8
1	3,363	24
2	3,589	40
3	3,712	58
4	3,775	84

Table S5: Counts of gene models predicted in *Volvox* by initial automated annotation, classified by method

The number of gene models that were generated with the automated JGI gene annotation pipeline are shown partitioned into the different methods that generated them. The gene models shown here are the raw output before genes with homology to Transposable Elements were filtered.

Method used to generate gene model	Number of gene models
Based on homology to proteins in nr database at GenBank	3,645 (23%)
<i>Ab initio</i> gene prediction	10,217 (67%)
Based on EST cluster consensuses	143 (1%)
Based on synteny with <i>C. reinhardtii</i>	1,539 (10%)
Total initial models	15,544 (100%)

Table S6. EST and homology evidence supporting initial *Volvox* and *Chlamydomonas* gene models

The numbers of gene models in the initial predictions that are complete from the start to the stop, have EST support or homology to a protein in Swissprot are shown. The models included in this table are those that were the output of the automated JGI annotation pipeline for *Volvox* and the frozen GeneCatalog (S14) that was submitted to GenBank (S8) (Accession ABCNoooooooo).

Evidence	<i>Volvox</i>	<i>Chlamydomonas</i>
Complete models	13,134 (85%)	8,919 (58%)
Models with EST alignment	5,356 (34%)	7,894 (51%)
Models with Swissprot alignment	10,947 (70%)	10,760 (71%)

Table S7: Gene structure statistics of *Volvox* and *Chlamydomonas* gene models

A variety of statistics are shown for the set of *Volvox* gene models after removing those with homology to Transposable Elements and the manually-curated set of *Chlamydomonas* gene models that were submitted to GenBank (S8) (Accession ABCN01000000).

	<i>Volvox</i>	<i>Chlamydomonas</i>
Protein-coding loci	14,520	14,516
Mean gene span (nt)	5,269	4,375
Total length of spliced transcripts (nt)	27,126,224	23,675,605
Mean transcript length (nt)	1,833	1,631
Mean protein length (aa)	568	454
Mean exon length (nt)	194	232
Mean intron length (nt) ¹	491	371
Mean no. exons	7.78	8.42

¹ Introns less than 20 nt long are ignored

* This is the set of gene models that was submitted to GenBank under the Accession ACJHoooooooo

Table S8: Comparison of *Volvox* genome statistics to selected other genomes.

Group	Species	Genome Size (Mb)	Number of chromosomes	%GC	Protein coding loci	% coding	% genes with introns	Introns per gene	Median intron length (bp)
CHLOROPHYTA	<i>Volvox carteri</i>	138	14*	56	14,520	18.0	92	7.05	358
	<i>Chlamydomonas reinhardtii</i>	118	17	64	14,516	16.3	91	7.4	174
STREPTOPHYTA	<i>Physcomitrella patens</i>	480	27	34	35,938	17.9	86	3.9	205
	<i>Arabidopsis thaliana</i>	140.1	5	36	26,541	23.7	80	4.4	55
OPISTHOKONTA	<i>Homo sapiens</i>	2851	23	41	23,328	1.2	83	7.8	20,383
	<i>Nematostella vectensis</i>	450	15	40	27,273	6.0	68	4.3	290
	<i>Monosiga brevicollis</i>	42	N.A.	55	9,196	39.4	89	6.6	135
	<i>Neurospora crassa</i>	40	7	54	10,107	36.4	80	1.7	72
AMOEBOZOA	<i>Dictyostelium discoideum</i>	34	6	22	13,574	62.2	68	1.3	236
CHROMALVEOLATA	<i>Thalassiosira pseudonana</i>	34.5	24	47	11,390	49.4	60	1.5	57

* see (S75)

N.A. not available

Table S9: Pfam domain counts and combinations in *Volvox* and *Chlamydomonas* compared to selected other species

	<i>Volvox</i>	<i>Chlamydomonas</i>	<i>Arabidopsis</i>	<i>Monosiga</i>	sea anemone	human
Total number of domains in proteome	10,318	10,168	38,887	11,786	30,535	42,057
No. different PFAM domains	2,431	2,354	3,028	2,232	3,078	3,832
No. different pairwise combinations	1,392	1,219	1,838	2,128	2,723	4,038
No. proteins with 1 domain	5,368	5,437	15,547	4,154	12,843	11,570
No. proteins with 2 domain types	989	880	3,639	1,157	2,456	3,543
No. proteins > 2 domain types	287	267	1,193	494	797	1,799

Table S10: Complete predicted protein sets used to build protein families

The genus and species, together with abbreviations used in e.g. Table S12 as well as their version and notes are shown for all proteomes used to make protein families (see above).

Species name	Abbreviation	Version and Notes
<i>Cyanidioschyzon merolae</i> 10D	Cme	release Apr 8, 2004; http://merolae.biol.s.u-tokyo.ac.jp/download
<i>Synechocystis</i> sp. PCC 6803	Syn	complete genome - 0..3573470 GenBank Accession NC_000911
<i>Pseudomonas aeruginosa</i> PA01	Pae	complete genome - 0..6264403 GenBank Accession NC_002516
<i>Staphylococcus aureus</i> subsp. <i>aureus</i> N315	Sau	complete genome - 0..2814816 GenBank Accession NC_002745
<i>Dictyostelium discoideum</i>	Ddi	dictyBase.org; Full Chromosomes made 10/05/2004; Primary Features made 7/11/2005
<i>Tetrahymena thermophila</i> SB210	Tth	<i>Tetrahymena</i> Genome Database (TIGR) Aug 2004
<i>Phytophthora ramorum</i>	Pra	JGI v.1 http://genome.jgi-psf.org/Phyra1_1/Phyra1_1.home.html
<i>Phytophthora sojae</i>	Pso	JGI v.1 http://genome.jgi-psf.org/sojae1/sojae1.home.html

<i>Neurospora crassa</i>	Ncr	http://funal.genome.duke.edu , genome_neurospora_crassa.20020212.nt.gz
<i>Prochlorococcus marinus</i> str. MIT9313	Pma	2003 JGI/ORNL http://genome.jgi-psf.org/prom9/prom9.home.html
<i>Arabidopsis thaliana</i>	Ath	TAIR6, updated 11.2005 from NCBI ftp://ftp.ncbi.nih.gov/genomes/Arabidopsis_thaliana
<i>Homo sapiens</i>	Hsa	NCBI 36 from ensembl build 38
<i>Caenorhabditis elegans</i>	Cel	WS 150 from ensembl build 38
<i>Ostreococcus tauri</i>	Ota	JGI v2.0 http://genome.jgi-psf.org/Ostta4/Ostta4.home.html
<i>Ostreococcus lucimarinus</i>	Olu	(<i>O. pacifica</i> ; <i>Ostreococcus</i> CCE9901) JGI v. 2.0 http://genome.jgi-psf.org/Ost9901_3/Ost9901_3.home.html
<i>Physcomitrella patens</i>	Ppa	JGI v. 1 http://genome.jgi-psf.org/Phypa1_1/Phypa1_1.download.ftp.html
<i>Monosiga brevicollis</i>	Mbr	JGI v. 1 http://genome.jgi-psf.org/Monbr1/Monbr1.home.html
<i>Thalassiosira pseudonana</i>	Tps	JGI v. 3.0 http://genome.jgi-psf.org/Thaps3/Thaps3.home.html
<i>Naegleria gruberi</i>	Ngr	JGI v.1 http://genome.jgi-psf.org/Naegr1/Naegr1.home.html
<i>Paramecium tetraurelia</i>	Pte	peptides from macronuclear genome downloaded from Paramecium DB release date 28-MCH-2007
<i>Chlamydomonas reinhardtii</i>	Cre	JGI v.3.1 freeze for GenBank submission 9/13/2007 from http://genome.jgi-psf.org/Chlre4/Chlre4.download.ftp.html
<i>Volvox carteri</i>	Vca	JGI v1 freeze from http://genome.jgi-psf.org/Volca1/Volca1.download.ftp.html

Table S11: Protein family size distribution in *Volvox* and *Chlamydomonas*

The number of protein families containing 1, 2-5 or more than 5 proteins from *Chlamydomonas* (columns across) and *Volvox* (rows down) are shown.

	<i>Chlamydomonas</i> proteins in family		
<i>Volvox</i> proteins in family	1	2-5	>5
1	5,423	295	2
2-5	282	669	13
>5	10	19	33

Table S12: *Volvox*-specific gene models with EST evidence

Presence of EST support and its quality is shown as counts of putative *Volvox*-specific genes that either have homology to another putative *Volvox*-specific gene (left column) or do not have such homology (right column), suggesting that these proteins might belong to *Volvox*-specific families, or might represent singleton *Volvox*-specific proteins respectively.

Does protein have a hit to another putative <i>Volvox</i> -specific protein?	yes	no
Full-length EST support	16	9
EST support over part of the gene model	11	0
Problem with EST support	57	47
Total	84	58

Table S13: *Chlamydomonas*-specific gene models with EST support

Presence of EST support and its quality is shown as fractions of a random sample of putative *Chlamydomonas*-specific genes that either have homology to another putative *Chlamydomonas*-specific gene (left column) or do not have such homology (right column), suggesting that these proteins might belong to *Chlamydomonas*-specific families, or might represent singleton *Chlamydomonas*-specific proteins respectively.

Does protein have a hit to another putative <i>Chlamydomonas</i> -specific protein?	Yes	No
Consistent EST support	32 %	60 %
EST probably supports gene model	30 %	16 %
Problem with EST support	38 %	24%

Table S14: Proteins involved in processes that are associated with increased developmental complexity in *Volvox* relative to *Chlamydomonas*

In the table, the names given are gene symbols, with synonyms given after a forward slash. Symbols of paralogs/co-orthologs are separated by semi-colons. The JGI protein ID and defline are given in the next two columns. The following columns show information for *Chlamydomonas* (co-)orthologs. Where there is no gene symbol and protein ID in a column, a homolog could not be found. The ID of the protein family the proteins belong to is shown after the *Chlamydomonas* defline and is followed by abbreviations of all the species that have a member in that protein family. If the protein does not belong to a family, this column shows 'unclustered'. The abbreviations used are as follows: Cme, *Cyanidioschyzon merolae*; Syn, *Synechocystis* sp.; Pae, *Pseudomonas aeruginosa*; Sau, *Staphylococcus aureus*; Ddi, *Dictyostelium discoideum*; Tth, *Tetrahymena thermophila*; Pra, *Phytophthora ramorum*; Pso, *Phytophthora sojae*; Ncr, *Neurospora crassa*; Pma, *Prochlorococcus marinus*; Ath, *Arabidopsis thaliana*; Hsa, *Homo sapiens*; Cel, *Caenorhabditis elegans*; Ota, *Ostreococcus tauri*; Olu, *Ostreococcus lucimarinus*; Ppa, *Physcomitrella patens*; Mbr, *Monosiga brevicollis*; Tps, *Thalassiosira pseudonana*; Ngr, *Naegleria gruberi*; Pte, *Paramecium tetraurelia*; Cre, *Chlamydomonas reinhardtii*; Vca, *Volvox carteri*.

Table S12
volvox protein

TubB	75910 77081	beta tubulin (tubB2)	TUB1	TUB2	129876 129868	129876 129868	Aug.Cre:12.9542250;	Aug.Cre:12.9549550;	beta tubulin 1. beta tubulin 2	6571720	Cine.Dit.Th.Pso.Ncr.Ath.Hsa.Cel.Ota.Ota.Psa.Mbr.Tps.Ncr.Pte.Cre.Vca
TubG	80553	Gamma tubulin	TUG1	UNJ3	188933	188933	Aug.Cre:06.9299300;	Aug.Cre:06.9299300;	Gamma tubulin was TUG	6572302	Cine.Dit.Th.Pso.Ncr.Ath.Hsa.Cel.Ota.Ota.Psa.Mbr.Tps.Ncr.Pte.Cre.Vca
Tubb	60395	Delta tubulin	UNJ3	186082	186082	186082	Aug.Cre:05.9187350;	Aug.Cre:05.9187350;	delta tubulin	6572459	Not.Cre.Vca
Tubb	116596	Eta tubulin	TOH1	TOH1	154376	154376	Aug.Cre:05.9513450;	Aug.Cre:05.9513450;	Eta tubulin was TUH	6572484	Not.Cre.Vca
Tubb	56250	Epsilon tubulin	TOE1	TOE1	188195	188195	Aug.Cre:05.9172650;	Aug.Cre:05.9172650;	Epsilon tubulin was TUE	6572484	Not.Cre.Vca
centro-Zeta	109845 669937	putative centrin	VELZ/CENI	VELZ/CENI	159554	159554	Aug.Cre:11.0468450;	Aug.Cre:11.0468450;	centrin catalytic subunit 60 kDa	6572712	Thi.Pra.Pso.Ath.Hsa.Cel.Ota.Ota.Psa.Mbr.Tps.Ncr.Pte.Cre.Vca
KatA	82654	cathepsin 50 catalytic subunit 60 kDa	KAT1	KAT1	53314	53314	Aug.Cre:01.9427600;	Aug.Cre:01.9427600;	cathepsin 50 catalytic subunit was 54 kDa	6574521	Thi.Pra.Pso.Ath.Hsa.Cel.Ota.Ota.Psa.Mbr.Tps.Ncr.Pte.Cre.Vca
KatB	76999	cathepsin 50 catalytic subunit	VPS4	VPS4	98650	98650	Aug.Cre:01.94464400;	Aug.Cre:01.94464400;	cathepsin 50 catalytic subunit was 54 kDa	6572037	Thi.Pra.Pso.Ath.Hsa.Cel.Ota.Ota.Psa.Mbr.Tps.Ncr.Pte.Cre.Vca
KatC	94919	microtubule severing protein centrin p50 subunit	PF15	80954	80954	80954	Aug.Cre:05.916450;	Aug.Cre:05.916450;	unclustered	6573852	Pr.Pso.Ath.Hsa.Cel.Ota.Ota.Psa.Mbr.Tps.Ncr.Pte.Cre.Vca
Map1	99065	microtubule associated protein MAP65	TOGL	175143	175143	175143	Aug.Cre:05.9149850;	Aug.Cre:05.9149850;	Microtubule associated protein	6572022	Cine.Dit.Th.Pso.Ncr.Ath.Hsa.Cel.Ota.Ota.Psa.Mbr.Tps.Ncr.Pte.Cre.Vca
Mora	121331	microtubule organizing protein MAP65	MAP65	193464	394462	394462	Aug.Cre:13.9614050;	Aug.Cre:13.9614050;	microtubule interacting protein	6575395	Pr.Pso.Ath.Hsa.Cel.Ota.Ota.Psa.Mbr.Tps.Ncr.Pte.Cre.Vca
map65	120144	microtubule-associated protein MAP65	EBP1/EB1	194209	194209	194209	Aug.Cre:05.9741200;	Aug.Cre:05.9741200;	microtubule plus-end binding protein	6573189	Cine.Dit.Th.Pso.Ncr.Ath.Hsa.Cel.Ota.Ota.Psa.Mbr.Tps.Ncr.Pte.Cre.Vca
EB1	107043	microtubule plus-end binding protein EB1	CLASP	206206	206206	206206	Aug.Cre:05.9415700;	Aug.Cre:05.9415700;	CLIP-associated protein	6572528	Thi.Pra.Pso.Ath.Ncr.Hsa.Cel.Ota.Ota.Psa.Mbr.Ncr.Cre.Vca
Clasp	120833	CLIP-associated protein									
Spir1	103526	putative cortical microtubule associated protein	SPR1	191409	416188	416188	Aug.Cre:02.9130150;	Aug.Cre:02.9130150;	putative cortical microtubule associated protein	6571789	Pr.Pso.Ota.Ota.Pte.Cre.Vca
Spir1	110511	SPR1	GCP2	1507172	1507172	1507172	Aug.Cre:02.91525500;	Aug.Cre:02.91525500;	Gamma tubulin interacting protein	6576345	Dot.Th.Pra.Pso.Ncr.Ath.Hsa.Cel.Ota.Ota.Psa.Mbr.Tps.Ncr.Pte.Cre.Vca
GCP3	97867	gamma tubulin interacting protein	GCP3	152585	152585	152585	Aug.Cre:02.9764400;	Aug.Cre:02.9764400;	Gamma tubulin interacting protein	6576345	Dot.Th.Pra.Pso.Ncr.Ath.Hsa.Cel.Ota.Ota.Psa.Mbr.Tps.Ncr.Pte.Cre.Vca
GCP4	118030	gamma tubulin interacting protein	GCP4	146323	146323	146323	Aug.Cre:01.919150;	Aug.Cre:01.919150;	Gamma tubulin interacting protein	6573545	Dot.Th.Pra.Pso.Ncr.Ath.Hsa.Cel.Ota.Ota.Psa.Mbr.Tps.Ncr.Pte.Cre.Vca
Pida	99461	putative M1 associated signaling protein phospholipase D	P.D1	1904033	1904033	1904033	Aug.Cre:13.9591900;	Aug.Cre:13.9591900;	putative M1 associated signaling protein	6572358	Pr.Pso.Ota.Ota.Pte.Cre.Vca
D1HIC	92778	Cytoskeletal domain 1b in intermediate chain D1HIC	T1E	130394	130394	130394	Aug.Cre:02.9130900;	Aug.Cre:02.9130900;	Cytoskeletal domain 1b in light intermediate chain D1HIC	6572451	Thi.Pra.Pso.Ota.Ota.Pte.Cre.Vca
D1HIC	64869	microtubule severing protein centrin p50 subunit	T1E	240059	240059	240059	Aug.Cre:02.9130900;	Aug.Cre:02.9130900;	microtubule severing protein centrin p50 subunit	6571949	Dot.Th.Pra.Pso.Ncr.Ath.Hsa.Cel.Ota.Ota.Psa.Mbr.Tps.Ncr.Pte.Cre.Vca
ASD	121266	microtubule-associated protein ASD	ASD	150686	150686	150686	Aug.Cre:05.9281150;	Aug.Cre:05.9281150;	abnormal spindle protein	6572164	Dot.Th.Pra.Pso.Ncr.Ath.Hsa.Cel.Ota.Ota.Psa.Mbr.Tps.Ncr.Pte.Cre.Vca
T1A	73667	tubulin tubroline lase	T1L	115172	402156	402156	Aug.Cre:05.9329150;	Aug.Cre:05.9329150;	tubulin tubroline lase	6572224	Cine.Ssp.Pad.Dit.Th.Pso.Ncr.Ath.Hsa.Cel.Ota.Ota.Psa.Mbr.Tps.Ncr.Pte.Cre.Vca
T1B	52059	tubulin tubroline lase	T1L	170153	401190	401190	Aug.Cre:05.9301250;	Aug.Cre:05.9301250;	tubulin tubroline lase	6573545	Dot.Th.Pra.Pso.Ncr.Ath.Hsa.Cel.Ota.Ota.Psa.Mbr.Tps.Ncr.Pte.Cre.Vca
T1C	30444	tubulin tubroline lase	T1L	100160	100160	100160	Aug.Cre:05.9301250;	Aug.Cre:05.9301250;	tubulin tubroline lase	6573545	Dot.Th.Pra.Pso.Ncr.Ath.Hsa.Cel.Ota.Ota.Psa.Mbr.Tps.Ncr.Pte.Cre.Vca
T1D	105441	tubulin tubroline lase	T1L	119250	119250	119250	Aug.Cre:05.9301250;	Aug.Cre:05.9301250;	tubulin tubroline lase	6572234	Dot.Th.Pra.Pso.Ncr.Ath.Hsa.Cel.Ota.Ota.Psa.Mbr.Tps.Ncr.Pte.Cre.Vca
T1E	107180	tubulin tubroline lase	T1L	190829	513952	513952	Aug.Cre:12.9547700;	Aug.Cre:12.9547700;	tubulin tubroline lase	6572382	Thi.Pra.Pso.Ota.Ota.Pte.Cre.Vca
T1F	63077	tubulin tubroline lase	T1L	146893	146893	146893	Aug.Cre:01.9050450;	Aug.Cre:01.9050450;	tubulin tubroline lase	6571683	Pr.Mbr.Cre.Vca
T1G	99465	tubulin tubroline lase	T1L	190398	190398	190398	Aug.Cre:01.9050450;	Aug.Cre:01.9050450;	tubulin tubroline lase	6570722	Thi.Pso.Ota.Ota.Pte.Cre.Vca
T1H	10470	tubulin tubroline lase	T1L	176529	417767	417767	Aug.Cre:02.9120750;	Aug.Cre:02.9120750;	tubulin tubroline lase	6571683	unclustered
Bardet-Biedl Syndrome 5			BBS5	182299	182299	182299	Aug.Cre:06.9267550;	Aug.Cre:06.9267550;	Bardet-Biedl syndrome 5 protein	6570754	Thi.Pra.Pso.Ota.Ota.Pte.Cre.Vca
DOS5	78957	Bardet-Biedl syndrome 5	SFA	172795	172795	172795	Aug.Cre:05.932950;	Aug.Cre:05.932950;	SFA-assembly SF-assembly	6571809	Pr.Pso.Ota.Ota.Pte.Cre.Vca
DOS8	84701	putative RBP for filodendrin function	BBS8	140113	140113	140113	Aug.Cre:05.940054;	Aug.Cre:05.940054;	filodendrin	6571809	Pr.Pso.Ota.Ota.Pte.Cre.Vca
BBS4	65874	Bardet-Biedl syndrome protein 4	BBS4	192948	192948	192948	Aug.Cre:05.9486550;	Aug.Cre:05.9486550;	Bardet-Biedl syndrome 7 protein	6571791	Dot.Th.Pra.Pso.Ota.Ota.Pte.Cre.Vca
BBS4	70270	small Arf-related G-Pase	BBS4	244745	244745	244745	Aug.Cre:05.9486550;	Aug.Cre:05.9486550;	Bardet-Biedl syndrome protein 3B	6571791	Dot.Th.Pra.Pso.Ota.Ota.Pte.Cre.Vca
BBS2	121654	Bardet-Biedl syndrome protein 2	BBS2	127378	167558	167558	Aug.Cre:05.9486550;	Aug.Cre:05.9486550;	Bardet-Biedl syndrome protein 2	6571791	Dot.Th.Pra.Pso.Ota.Ota.Pte.Cre.Vca
BBS5	84705	Bardet-Biedl syndrome protein 1	BBS5	125317	125317	125317	Aug.Cre:05.9486550;	Aug.Cre:05.9486550;	Bardet-Biedl syndrome protein 1	6571791	Dot.Th.Pra.Pso.Ota.Ota.Pte.Cre.Vca
Q101	90133	bipolar body protein	QD1	31640	31640	31640	Aug.Cre:17.9730600;	Aug.Cre:17.9730600;	bipolar body protein	6576552	Thi.Pra.Pso.Ota.Ota.Pte.Cre.Vca
V13	84510	protein conserved only in onychists with motile cilia	VFL3	130542	130542	130542	Aug.Cre:06.92729900;	Aug.Cre:06.92729900;	protein required for templated centrole	6572787	Thi.Pra.Pso.Ota.Ota.Pte.Cre.Vca
Q101	57976	bipolar body protein	BLD10	166062	166062	166062	Aug.Cre:01.9418250;	Aug.Cre:01.9418250;	bipolar body protein	6573246	Dot.Th.Pra.Pso.Ota.Ota.Pte.Cre.Vca
bbs9	119731	Bardet-Biedl syndrome 9	BBS9	101137	101137	101137	Aug.Cre:02.9107090;	Aug.Cre:02.9107090;	Bardet-Biedl syndrome 9 protein	6572322	Thi.Pra.Pso.Ota.Ota.Pte.Cre.Vca
Kinesin Motor Proteins			Kinesin	191502	185750	185750	Aug.Cre:17.9418950;	Aug.Cre:17.9418950;	Kinesin family protein	6572333	unclustered
fla1	93532	Kinesin-like protein	FLA10	187750	187750	187750	Aug.Cre:05.9418950;	Aug.Cre:05.9418950;	Kinesin motor subunit	6572333	Cine.Dit.Th.Pra.Pso.Ncr.Ath.Hsa.Cel.Ota.Ota.Psa.Mbr.Tps.Ncr.Pte.Cre.Vca
fla1/kipd5	107307	Kinesin-like protein	FLA8	187666	187666	187666	Aug.Cre:17.9422550;	Aug.Cre:17.9422550;	Kinesin family member heavy chain	6574543	Cine.Dit.Th.Pra.Pso.Ncr.Ath.Hsa.Cel.Ota.Ota.Psa.Mbr.Tps.Ncr.Pte.Cre.Vca
kipd5	103736	putative Kinesin-like protein	KIP1	137433	137433	137433	Aug.Cre:05.9418950;	Aug.Cre:05.9418950;	Kinesin-like protein	6572085	unclustered
KIP1	92813	Kinesin-like protein similar to C. reinhardtii KIP1	KIP1	186114	186114	186114	Aug.Cre:07.37550;	Aug.Cre:07.37550;	Kinesin-like protein	6572111	unclustered
KIF6	94698	KIF6 type kinesin-like protein	KIF6	186225	186225	186225	Aug.Cre:10.9418950;	Aug.Cre:10.9418950;	Kinesin family protein	6572334	unclustered
InvA	122792	Kinesin-like protein	TAIR1	126081	126081	126081	Aug.Cre:10.9418950;	Aug.Cre:10.9418950;	Kinesin family protein	6572334	unclustered
KIF10	122741	Kinesin-like protein	KIF10	145399	149713	149713	Aug.Cre:09.9386700;	Aug.Cre:09.9386700;	Kinesin motor protein	6572334	unclustered
KIF10	122742	Kinesin-like protein	KIF10	137433	137433	137433	Aug.Cre:09.9418950;	Aug.Cre:09.9418950;	Kinesin motor protein	6572334	unclustered
KIF10	122743	Kinesin-like protein	KIF10	187496	188266	188266	Aug.Cre:09.9418950;	Aug.Cre:09.9418950;	Kinesin motor protein	6572334	unclustered
KIF10	122744	Kinesin-like protein	KIF10	147352	148888	148888	Aug.Cre:09.9418950;	Aug.Cre:09.9418950;	Kinesin motor protein	6572334	unclustered
KIF10	122745	Kinesin-like protein	KIF10	139268	140755	140755	Aug.Cre:09.9418950;	Aug.Cre:09.9418950;	Kinesin motor protein	6572334	unclustered
KIF10	122746	Kinesin-like protein	KIF10	147353	147353	147353	Aug.Cre:09.9418950;	Aug.Cre:09.9418950;	Kinesin motor protein	6572334	unclustered
KIF10	122747	Kinesin-like protein	KIF10	147354	147354	147354	Aug.Cre:09.9418950;	Aug.Cre:09.9418950;	Kinesin motor protein	6572334	unclustered
KIF10	122748	Kinesin-like protein	KIF10	147355	147355	147355	Aug.Cre:09.9418950;	Aug.Cre:09.9418950;	Kinesin motor protein	6572334	unclustered
KIF10	122749	Kinesin-like protein	KIF10	147356	147356	147356	Aug.Cre:09.9418950;	Aug.Cre:09.9418950;	Kinesin motor protein	6572334	unclustered
KIF10	122750	Kinesin-like protein	KIF10	147357	147357	147357	Aug.Cre:09.9418950;	Aug.Cre:09.9418950;	Kinesin motor protein	6572334	unclustered
KIF10	122751	Kinesin-like protein	KIF10	147358	147358	147358	Aug.Cre:09.9418950;	Aug.Cre:09.9418950;	Kinesin motor protein	6572334	unclustered
KIF10	122752	Kinesin-like protein	KIF10	147359	147359	147359	Aug.Cre:09.9418950;	Aug.Cre:09.9418950;	Kinesin motor protein	6572334	unclustered
KIF10	122753	Kinesin-like protein	KIF10	147360	147360	147360	Aug.Cre:09.9418950;	Aug.Cre:09.9418950;	Kinesin motor protein	6572334	unclustered
KIF10	122754	Kinesin-like protein	KIF10	147361	147361	147361	Aug.Cre:09.9418950;	Aug.Cre:09.9418950;	Kinesin motor protein	6572334	unclustered
KIF10	122755	Kinesin-like protein	KIF10	147362	147362	147362	Aug.Cre:09.9418950;	Aug.Cre:09.9418950;	Kinesin motor protein	6572334	unclustered
KIF10	122756	Kinesin-like protein	KIF10	147363	147363	147363	Aug.Cre:09.9418950;	Aug.Cre:09.9418950;	Kinesin motor protein	6572334	unclustered
KIF10	122757	Kinesin-like protein	KIF10	147364	147364	147364	Aug.Cre:09.9418950;	Aug.Cre:09.9418950;	Kinesin motor protein	6572334	unclustered
KIF10	122758	Kinesin-like protein	KIF10	147365	147365	147365	Aug.Cre:09.9418950;	Aug.Cre:09.9418950;	Kinesin motor protein	6572334	unclustered
KIF10	122759	Kinesin-like protein	KIF10	147366	147366	147366	Aug.Cre:09.9418950;	Aug.Cre:09.9418950;	Kinesin motor protein	6572334	unclustered
KIF10	122760	Kinesin-like protein	KIF10	147367	147367	147367	Aug.Cre:09.9418950;	Aug.Cre:09.9418950;	Kinesin motor protein	6572334	unclustered
KIF10	122761	Kinesin-like protein	KIF10	147368	147368	147368	Aug.Cre:09.9418950;	Aug.Cre:09.9418950;	Kinesin motor protein	6572334	unclustered
KIF10	122762	Kinesin-like protein	KIF10	147369	147369	147369	Aug.Cre:09.9418950;	Aug.Cre:09.9418950;	Kinesin motor protein	6572334	unclustered
KIF10	122763	Kinesin-like protein	KIF10	147370	147370	147370	Aug.Cre:09.9418950;	Aug.Cre:09.9418950;	Kinesin motor protein	6572334	unclustered
KIF10	122764	Kinesin-like protein	KIF10	147371	147371	147371	Aug.Cre:09.9418950;	Aug.Cre			

phiI	85077	extracellular matrix glycoprotein phosphophitin II	6574211	Cre Vca
phiII	83859	extracellular matrix glycoprotein phosphophitin III	unclustered	unclustered
phiIS	104453	extracellular matrix glycoprotein phosphophitin-D21	unclustered	unclustered
phiB21	77905	extracellular matrix glycoprotein phosphophitin-D22	unclustered	unclustered
phiB22	90188	extracellular matrix glycoprotein phosphophitin-VI	unclustered	unclustered
phiV1	77332	extracellular matrix glycoprotein phosphophitin-V2	unclustered	unclustered
phiV2	108351	extracellular matrix glycoprotein phosphophitin-V3	unclustered	unclustered
phiV3	110102	extracellular matrix glycoprotein phosphophitin-V4	unclustered	unclustered
phiV4	77335	extracellular matrix glycoprotein phosphophitin-V5	unclustered	unclustered
phiV5	77338	extracellular matrix glycoprotein phosphophitin-V6	unclustered	unclustered
phiV6	107455	extracellular matrix glycoprotein phosphophitin-V7	unclustered	unclustered
phiV7	108791	extracellular matrix glycoprotein phosphophitin-V8	unclustered	unclustered
phiV8	63512	extracellular matrix glycoprotein phosphophitin-V9 (Env955)	unclustered	unclustered
phiV9	75691	extracellular matrix glycoprotein phosphophitin-V9	unclustered	unclustered
phiV10	104451	extracellular matrix glycoprotein phosphophitin-V10	unclustered	unclustered
phiV11	104452	extracellular matrix glycoprotein phosphophitin-V11	unclustered	unclustered
phiV12	59555	extracellular matrix glycoprotein phosphophitin-V12	unclustered	unclustered
phiV13	127206	extracellular matrix glycoprotein phosphophitin-V13	unclustered	unclustered
phiV14	80812	extracellular matrix glycoprotein phosphophitin-V14	unclustered	unclustered
phiV15	80731	extracellular matrix glycoprotein phosphophitin-V15	unclustered	unclustered
phiV16	78132	extracellular matrix glycoprotein phosphophitin-V16	unclustered	unclustered
phiV17	101178	extracellular matrix glycoprotein phosphophitin-V17	unclustered	unclustered
phiV18	80872	extracellular matrix glycoprotein phosphophitin-V18 (Env1955)	unclustered	unclustered
phiV19	83847	extracellular matrix glycoprotein phosphophitin-V19 (Env1955)	unclustered	unclustered
phiV20	42640	extracellular matrix glycoprotein phosphophitin-V20	unclustered	unclustered
phiV21	90431	extracellular matrix glycoprotein phosphophitin-V21	unclustered	unclustered
phiV22	94616	extracellular matrix glycoprotein phosphophitin-V22	unclustered	unclustered
phiV23	94560	extracellular matrix glycoprotein phosphophitin-V23	unclustered	unclustered
phiV24	127208	extracellular matrix glycoprotein phosphophitin-V24	unclustered	unclustered
phiV25	101351	extracellular matrix glycoprotein phosphophitin-V25	unclustered	unclustered
phiV26	107546	extracellular matrix glycoprotein phosphophitin-V26 (similar to Chitamandosin, Gm30)	unclustered	unclustered
phiV27	67890	extracellular matrix glycoprotein phosphophitin-V27 (similar to Chitamandosin, Gm30)	unclustered	unclustered
phiV28	77438	extracellular matrix glycoprotein phosphophitin-V28 (similar to Chitamandosin, Gm30)	unclustered	unclustered
phiV29	67883	extracellular matrix glycoprotein phosphophitin-V29 (similar to Chitamandosin, Gm30)	unclustered	unclustered
phiV30	67897	extracellular matrix glycoprotein phosphophitin-V30 (similar to Chitamandosin, Gm30)	unclustered	unclustered
phiV31	104151	extracellular matrix glycoprotein phosphophitin-V31 (similar to Chitamandosin, Gm30)	unclustered	unclustered
phiV32	104390	extracellular matrix glycoprotein phosphophitin-V32 (similar to Chitamandosin, Gm30)	unclustered	unclustered
phiV33	95611	extracellular matrix glycoprotein phosphophitin-V33	unclustered	unclustered
phiV34	107649	extracellular matrix glycoprotein phosphophitin-V34	unclustered	unclustered
phiV35	127252	extracellular matrix glycoprotein phosphophitin-V35	unclustered	unclustered
phiV36	89822	extracellular matrix glycoprotein phosphophitin-V36	unclustered	unclustered
phiV37	127212	extracellular matrix glycoprotein phosphophitin-V37	unclustered	unclustered
phiV38	55073	extracellular matrix glycoprotein phosphophitin-V38	unclustered	unclustered
phiV39	100779	extracellular matrix glycoprotein phosphophitin-V39	unclustered	unclustered
phiV40	106281	extracellular matrix glycoprotein phosphophitin-V40	unclustered	unclustered
phiV41	97824	extracellular matrix glycoprotein phosphophitin-V41	unclustered	unclustered
phiV42	90414	extracellular matrix glycoprotein phosphophitin-V42 (Chromosomes Phrcohortin Hormolos)	unclustered	unclustered
phiC1	196399	196399	A19_Cre17_017179000	cell wall protein phosphochitin-C1
phiC2	196402	196402	A19_Cre17_023016500	cell wall protein phosphochitin-C2
phiC3	196403	196403	A19_Cre15_0586450	cell wall protein phosphochitin-C3
phiC4	196405	196405	A19_Cre15_0545000	cell wall protein phosphochitin-C4
phiC5	196406	196406	A19_Cre05_0280000	cell wall protein phosphochitin-C5
phiC6	196407	196407	A19_Cre17_0171800	cell wall protein phosphochitin-C6
phiC7	195907	195907	A19_Cre17_0171800	cell wall protein phosphochitin-C7
phiC8	196005	196005	A19_Cre17_0171780	cell wall protein phosphochitin-C8
phiC9	196020	196020	A19_Cre06_0293150	cell wall protein phosphochitin-C9
phiC10	196024	196024	A19_Cre06_0401150	cell wall protein phosphochitin-C10
phiC11	196027	196027	A19_Cre07_0311150	cell wall protein phosphochitin-C11
phiC12	196264	196264	A19_Cre11_047272200	cell wall protein phosphochitin-C12
phiC13	304232	304232	A19_Cre11_047272200	cell wall protein phosphochitin-C13
phiC14	196029	196029	A19_Cre14_0620650	cell wall protein phosphochitin-C14
phiC15	536129	148233	A19_Cre09_039611000	cell wall protein phosphochitin-C15
phiC16	141201	141191	A19_Cre02_027388000	cell wall protein phosphochitin-C16
phiC17	522381	522381	A19_Cre05_027388050	cell wall protein phosphochitin-C17
phiC18	180163	180163	A19_Cre17_046955000	cell wall protein phosphochitin-C18
phiC19	196022	196022	A19_Cre09_0382150	cell wall protein phosphochitin-C19
phiC20	93464	93464	A19_Cre05_0309450	cell wall protein phosphochitin-C20
phiC21	94192	94192	A19_Cre17_046967000	cell wall protein phosphochitin-C21
phiC22	196023	196023	A19_Cre09_0382150	cell wall protein phosphochitin-C22
phiC23	196019	196019	A19_Cre09_0382150	cell wall protein phosphochitin-C23
phiC24	196025	196025	A19_Cre09_0382150	cell wall protein phosphochitin-C24
phiS28	192908	192908	A19_Cre11_0481600	hydroxyproline-rich glycoprotein, stress-
phiS30	195828	195828	A19_Cre11_0481750	induced
phiS31	193780	193780	A19_Cre45_0789350	cell wall protein phosphochitin
Sex-inducer	83768	sex-inducer, sex-inducing pheromone	unclustered	unclustered
sex1				

Table S15: Predicted numbers of TAPs

The number of proteins that were predicted in each Transcription Associated Protein (TAP) family in *Volvox* and *Chlamydomonas* are shown.

TAP	<i>Volvox</i>	<i>Chlamydomonas</i>
ABI3/VP1	1	1
Alfin-like	1	1
AP2/EREBP	21	12
ARF	0	0
Argonaute	2	3
ARID	2	3
AS2/LOB	0	0
Aux/IAA	0	0
BBR/BPC	0	0
BES1	0	0
bHLH	2	3
bHSH	0	0
BSD domain containing	3	1
bZIP	11	6
C2C2_CO-like	2	1
C2C2_Dof	1	1
C2C2_GATA	9	8
C2C2_YABBY	0	0
C2H2	8	6
C3H	23	15
CAMTA	0	0
CCAAT_Dr1	0	2
CCAAT_HAP2	0	0
CCAAT_HAP3	3	1
CCAAT_HAP5	2	2
Coactivator p15	1	1
CPP	2	1
CSD	2	1

CudA	0	0
DBP	0	0
DDT	0	0
Dicer	0	0
DUF246 domain containing	0	0
DUF296 domain containing	0	0
DUF547 domain containing	1	1
DUF632 domain containing	0	0
DUF833 domain containing	0	0
E2F/DP	3	3
EIL	0	0
FHA	11	12
GARP_G2-like	4	4
GARP_ARR-B	1	1
GeBP	0	0
GIF	1	1
GNAT	33	28
GRAS	0	0
GRF	0	0
HB	0	1
HB_KNOX	0	0
HD-Zip	0	0
HMG	9	7
HRT	0	0
HSF	2	2
IWS1	1	1
Jumonji	0	0
LFY	0	0
LIM	0	0
LUG	0	0
MADS	1	2
MBF1	1	1
MED6	0	1
MED7	1	0

mTERF	3	1
MYB-related	12	9
MYB	19	15
NAC	0	0
NZZ	0	0
OFP	0	0
PcG_EZ	0	0
PcG_FIE	1	1
PcG_VEFS	0	0
PHD	16	10
PLATZ	3	4
Pseudo ARR-B	0	2
RB	0	1
Rcd1-like	1	2
Rel	0	0
RF-X	0	0
RRN3	1	0
Runt	0	0
RWP-RK	9	14
S1Fa-like	0	0
SAP	0	0
SBP	20	21
SET	16	13
Sigma70-like	1	1
Sin3	1	1
Sir2	3	2
SOH1	1	0
SRS	0	0
SWI/SNF_BAF60b	1	2
SWI/SNF_SNF2	26	18
SWI/SNF_SWI3	0	0
TAZ	4	2
TCP	0	0
TEA	0	0

TFb2	0	1
TRAF	20	28
Trihelix	0	0
TUB	3	2
ULT	0	0
VARL	13	9
VOZ	0	0
Whirly	1	1
WRKY	2	1
zf_HD	0	0
tify	0	0
Zinc finger, AN1 and A20 type	2	1
Zinc finger, MIZ type	2	0
Zinc finger, ZPR1	1	1
Zn_clus	0	0
Total	347	297

Table S16: Summary of RepeatScout libraries

A summary of the number of repeat sequences (and their mean length) generated from running RepeatScout on the *Volvox* and *Chlamydomonas* assemblies is shown.

	<i>Volvox</i>	<i>Chlamydomonas</i>
Sequences in raw repeat library	1,511	1,057
Putative novel repeat sequences	122	58
Mean repeat sequence length	919	595
No. sequences left after removing unknown sequences with non-TE Pfam domains	1,449	1,013

5) SUPPLEMENTAL REFERENCES

- S1. C. R. Adams *et al.*, *Curr Genet* **18**, 141 (1990).
- S2. R. C. Starr, *Arch Protistenkd* **111**, 204 (1969).
- S3. R. C. Starr, *Dev Biol Suppl* **4**, 59 (1970).
- S4. D. R. Smith, R. W. Lee, *BMC Genomics* **10**, 132 (2009).
- S5. J. L. Weber, E. W. Myers, *Genome Res* **7**, 401 (May, 1997).
- S6. B. Ewing, L. Hillier, M. C. Wendl, P. Green, *Genome Res* **8**, 175 (Mar, 1998).
- S7. S. Aparicio *et al.*, *Science* **297**, 1301 (Aug 23, 2002).
- S8. D. A. Benson, I. Karsch-Mizrachi, D. J. Lipman, J. Ostell, E. W. Sayers, *Nucleic Acids Res* **37**, D26 (Jan, 2009).
- S9. W. J. Kent, *Genome Res* **12**, 656 (Apr, 2002).
- S10. S. F. Altschul, W. Gish, W. Miller, E. W. Myers, D. J. Lipman, *J Mol Biol* **215**, 403 (Oct 5, 1990).
- S11. T. U. Consortium, *Nucleic Acids Res* **38**, D142 (Jan, 2010).
- S12. A. F. A. Smit, R. Hubley, P. Green, <http://www.repeatmasker.org>, (1996-2004).
- S13. J. Jurka *et al.*, *Cytogenet Genome Res* **110**, 462 (2005).
- S14. S. S. Merchant *et al.*, *Science* **318**, 245 (Oct 12, 2007).
- S15. A. L. Price, N. C. Jones, P. A. Pevzner, *Bioinformatics* **21 Suppl 1**, i351 (Jun, 2005).
- S16. S. R. Eddy, *Bioinformatics* **14**, 755 (1998).
- S17. T. M. Lowe, S. R. Eddy, *Nucleic Acids Res* **25**, 955 (Mar 1, 1997).
- S18. E. Quevillon *et al.*, *Nucleic Acids Res* **33**, W116 (Jul 1, 2005).
- S19. G. A. Tuskan *et al.*, *Science* **313**, 1596 (Sep 15, 2006).
- S20. A. Coghlan, E. E. Eichler, S. G. Oliver, A. H. Paterson, L. Stein, *Trends Genet* **21**, 673 (Dec, 2005).
- S21. J. C. Detter *et al.*, *Genomics* **80**, 691 (Dec, 2002).
- S22. B. Ewing, P. Green, *Genome Res* **8**, 186 (Mar, 1998).
- S23. T. G. I. Project.
- S24. X. Huang, A. Madan, *Genome Res* **9**, 868 (Sep, 1999).
- S25. A. Z. Worden *et al.*, *Science* **324**, 268 (Apr 10, 2009).
- S26. A. Y. Guo *et al.*, *Nucleic Acids Res* **36**, D966 (Jan, 2008).
- S27. D. M. Riano-Pachon, S. Ruzicic, I. Dreyer, B. Mueller-Roeber, *BMC Bioinformatics* **8**, 42 (2007).
- S28. S. Richardt, D. Lang, R. Reski, W. Frank, S. A. Rensing, *Plant Physiol* **143**, 1452 (Apr, 2007).
- S29. R. D. Finn *et al.*, *Nucleic Acids Res* **36**, D281 (Jan, 2008).
- S30. P. Perez-Rodriguez *et al.*, *Nucleic Acids Res* **38**, D822 (Jan, 2009).
- S31. K. Katoh, K. Kuma, H. Toh, T. Miyata, *Nucleic Acids Res* **33**, 511 (2005).
- S32. M. Clamp, J. Cuff, S. M. Searle, G. J. Barton, *Bioinformatics* **20**, 426 (Feb 12, 2004).
- S33. A. Sanderfoot, *Plant Physiol* **144**, 6 (May, 2007).

S34. S. Rutherford, I. Moore, *Curr Opin Plant Biol* **5**, 518 (Dec, 2002).

S35. J. D. Thompson, T. J. Gibson, F. Plewniak, F. Jeanmougin, D. G. Higgins, *Nucleic Acids Res* **25**, 4876 (Dec 15, 1997).

S36. R. C. Edgar, *Nucleic Acids Res* **32**, 1792 (2004).

S37. D. Swofford. (Sinauer Associates, Sunderland, MA, 2003).

S38. K. Bisova, D. M. Krylov, J. G. Umen, *Plant Physiol* **137**, 475 (Feb, 2005).

S39. M. Berriman *et al.*, *Science* **309**, 416 (Jul 15, 2005).

S40. A. Hallmann, *Int Rev Cytol* **227**, 131 (2003).

S41. E. H. Harris, Stern, D.B., and Witman, G.B., *The Chlamydomonas Sourcebook*. (Academic Press, 2009).

S42. F. Abascal, R. Zardoya, D. Posada, *Bioinformatics* **21**, 2104 (May 1, 2005).

S43. S. Guindon, O. Gascuel, *Syst Biol* **52**, 696 (Oct, 2003).

S44. S. Guindon, F. Lethiec, P. Duroux, O. Gascuel, *Nucleic Acids Res* **33**, W557 (Jul 1, 2005).

S45. E. Szathmary, J. M. Smith, *Nature* **374**, 227 (Mar 16, 1995).

S46. J. T. Bonner, *Integr Biol* **1**, 27 (1998).

S47. S. L. Baldauf, *Science* **300**, 1703 (Jun 13, 2003).

S48. R. K. Grosberg, R. Strathmann, *Annu Rev Ecol Evol Syst* **38**, 621 (2007).

S49. G. A. Wray, *Genome Biol* **3**, REVIEW0001 (2002).

S50. H. S. Yoon, J. D. Hackett, C. Ciniglia, G. Pinto, D. Bhattacharya, *Mol Biol Evol* **21**, 809 (May, 2004).

S51. M. D. Herron, J. D. Hackett, F. O. Aylward, R. E. Michod, *Proc Natl Acad Sci U S A* **106**, 3254 (Mar 3, 2009).

S52. H. Rausch, N. Larsen, R. Schmitt, *J Mol Evol* **29**, 255 (Sep, 1989).

S53. T. Nakada, K. Misawa, H. Nozaki, *Mol Phylogenet Evol* **48**, 281 (Jul, 2008).

S54. H. Nozaki, *Biologia, Bratislava* **58**, 425 (2003).

S55. S. M. Miller, D. L. Kirk, *Development* **126**, 649 (Feb, 1999).

S56. Q. Cheng, R. Fowler, L. W. Tam, L. Edwards, S. M. Miller, *Dev Genes Evol* **213**, 328 (Jul, 2003).

S57. I. Nishii, S. Ogihara, D. L. Kirk, *Cell* **113**, 743 (Jun 13, 2003).

S58. M. M. Kirk *et al.*, *Development* **126**, 639 (Feb, 1999).

S59. M. Meissner, K. Stark, B. Cresnar, D. L. Kirk, R. Schmitt, *Curr Genet* **36**, 363 (Dec, 1999).

S60. L. Duncan *et al.*, *J Mol Evol* **65**, 1 (Jul, 2007).

S61. H. Gruber, S. D. Goetinck, D. L. Kirk, R. Schmitt, *Gene* **120**, 75 (Oct 12, 1992).

S62. A. Hallmann, A. Rappel, *Plant J* **17**, 99 (Jan, 1999).

S63. T. Jakobiak *et al.*, *Protist* **155**, 381 (Dec, 2004).

S64. A. Hallmann, S. Wodniok, *Plant Cell Rep* **25**, 582 (Jun, 2006).

S65. S. M. Miller, R. Schmitt, D. L. Kirk, *Plant Cell* **5**, 1125 (Sep, 1993).

S66. N. Ueki, I. Nishii, *Genetics* **180**, 1343 (Nov, 2008).

S67. B. Schiedlmeier *et al.*, *Proc Natl Acad Sci U S A* **91**, 5080 (May 24, 1994).

S68. A. Hallmann, M. Sumper, *Eur J Biochem* **221**, 143 (Apr 1, 1994).

S69. D. L. Kirk, *Bioessays* **27**, 299 (Mar, 2005).

S70. P. Ferris *et al.*, *Science* **328**, 351 (Apr 16, 2010).

S71. A. Hallmann, K. Godl, S. Wenzl, M. Sumper, *Trends Microbiol* **6**, 185 (May, 1998).

S72. A. Hallmann, *Planta* **226**, 719 (Aug, 2007).

S73. N. Aono, T. Inoue, H. Shiraishi, *J Biochem* **138**, 375 (Oct, 2005).

S74. A. Hallmann, *Plant J* **45**, 292 (Jan, 2006).

S75. D. Kirk, *Volvox: Molecular-genetic origins of multicellularity and cellular differentiation*. (Cambridge University Press, Cambridge, 1998).

S76. D. Stern, G. Witman, E. Harris, (Jan 1, 2009).

S77. T. Kubo, J. Abe, T. Saito, Y. Matsuda, *Curr Genet* **41**, 115 (May, 2002).

S78. T. Hamaji *et al.*, *Genetics* **178**, 283 (Jan, 2008).

S79. H. Nozaki, T. Mori, O. Misumi, S. Matsunaga, T. Kuroiwa, *Curr Biol* **16**, R1018 (Dec 19, 2006).

S80. D. L. Kirk, R. Birchem, N. King, *J Cell Sci* **80**, 207 (Feb, 1986).

S81. R. R. Reisz, J. Muller, *Trends Genet* **20**, 237 (May, 2004).

S82. M. Goodman, G. W. Moore, G. Matsuda, *Nature* **253**, 603 (Feb 20, 1975).

S83. H. Wang *et al.*, *Proc Natl Acad Sci U S A* **106**, 3853 (Mar 10, 2009).

S84. C. Bowler *et al.*, *Nature* **456**, 239 (Nov 13, 2008).

LEGAL DISCLAIMER

This document was prepared as an account of work sponsored by the United States Government. While this document is believed to contain correct information, neither the United States Government nor any agency thereof, nor The Regents of the University of California, nor any of their employees, makes any warranty, express or implied, or assumes any legal responsibility for the accuracy, completeness, or usefulness of any information, apparatus, product, or process disclosed, or represents that its use would not infringe privately owned rights. Reference herein to any specific commercial product, process, or service by its trade name, trademark, manufacturer, or otherwise, does not necessarily constitute or imply its endorsement, recommendation, or favoring by the United States Government or any agency thereof, or The Regents of the University of California. The views and opinions of authors expressed herein do not necessarily state or reflect those of the United States Government or any agency thereof or The Regents of the University of California.